Politecnico di Torino

Master's Degree in Biomedical Engineering

GelMA-based hydrogels for 3D modeling of metastatic Colorectal Cancer patient-derived organoids

Supervisor: **Candidate:**

Dott.ssa Giulia MESIANO   Federica GEMIGNANI

July 2025

Table of Contents

Abstract

Gelatine methacryloyl (GelMA)-based hydrogels are emerging as innovative and promising 3D platforms, increasingly employed in many fields of biomedical research due to their high versatility, biocompatibility and tunability of mechanical properties. Derived from gelatine and functionalized with methacrylic anhydride, GelMA can be precisely tailored by adjusting set up synthesis, enabling the formation of highly customizable 3D matrices via photo-polymerization. This study aimed to assess the potential of GelMA-based hydrogel as a support for mimicking the extracellular matrix (ECM) of metastatic colorectal cancer (mCRC), the third most frequently diagnosed malignant tumour worldwide. Nowadays 3D in-vitro models are widely adopted to investigate the biological processes underlying pathologies as mCRC, and as platforms for the evaluation of new therapeutic agents, due to their ability to faithfully reproduce the 3D native tissue architecture. The first part of this thesis focused on establishing 3D cultures of mCRC in two different types of GelMA (Type A and B) and comparing the performance of these matrices with Matrigel, the current gold standard for 3D models due to its ECM-like properties. However, Matrigel presents several major drawbacks: high cost, batch-to-batch variability, limited tunability, and ethical concerns. GelMA Types A and B differ based on the source of the native gelatine used in their synthesis: porcine and bovine-derived respectively. In-vitro assays show that GelMA A-based matrix is more suitable for culturing metastatic tumour cell line (T84), exhibiting higher viability, morphological features and structural organizations comparable to those observed in Matrigel. To further assess the performance of GelMA A-based hydrogels, we had the valuable opportunity to work with primary biological material: five patient-derived mCRC organoids from the XENTURION Biobank platform, kindly provided by Prof. L. Trusolino. These organoids were generated from liver mCRC patients, KRAS/NRAS-mutated and resistant to conventional treatments. Moreover, patient-derived mCRC organoids show the same mutational profiles and drug sensitivity of the original tumours. The experiments were conducted with GelMA A-based hydrogels synthetized with different Degrees of Functionalization (DoF) and weight on volume (w/v) concentrations in the final solution (High DoF at 12,5% w/v, Medium DoF at 12,5%, 10%, and 7,5% w/v), while maintaining the other experimental parameters (light intensity of 365 nm, and time exposure of 45') constant. All the experiments were performed with Matrigel as reference. Morphological analyses, based on confocal spinning disk microscopy, and 3D proliferation assays over two weeks cultures, confirmed GelMA A-based hydrogels' effectiveness in preserving essential cellular functions and interactions. Subsequently, the composition of the matrices has been optimized to achieve mechanical properties and biocompatibility levels adequate to support patient-derived mCRC organoids proliferation and morphological

organization. Medium DoF at 7,5% w/v concentration of GelMA A results in the best performing formulation, highlighting it as a promising alternative to conventional materials for drug testing, personalized mCRC therapy and for the study of tumour dynamics. Potential future directions involve long-term cultures to investigate the transcriptome profile and drug response consistency between patient-derived mCRC organoids cultured in GelMA and original tumours.

Acknowledgements

1. Introduction

1.1. Colorectal cancer

Colorectal cancer (CRC) is a heterogeneous neoplastic disease determined by the malignant degeneration of the external epithelium of the large intestine [1]. In 2020, CRC has been classified as the second leading cancer cause associated with human death with 1.9 million new cases[2] and the third most frequently diagnosed malignant tumour worldwide [3]. The occurrence and the mortality of CRC depend on the distribution of risk factors particularly frequent in countries as Asia, characterised by the highest incidence of the disease itself (52,3%), and Europe (26,9%), followed by North America (9,3%), Latin America and Caribbean (7%), and finally Africa (3,4%) [3]. Despite the progress both in the diagnosis and treatment of CRC, according to the International Agency for Research on Cancer (IARC), by 2040 the mortality rate will increase by 73% while the number of new cases, especially among young adults, will rise by 63% [3].

Figure 1: Approximative worldwide CRC distribution.

Colorectal carcinogenesis is associated to several risk factors, for example cigarette smoking, which is responsible for approximately 12% of CRC-related deaths [4]. Lifestyle plays a key role in the development of this type of disease: several studies have in fact shown that there is a strong correlation between sedentariness, lack of physical activity, and the possibility to develop CRC. Aerobic exercises seem to be helpful strategies to reduce the insurgence of digestive system

cancers, together with a well-balanced diet. Moreover, reducing the consumption of fatty foods and alcoholic beverages can decrease the risk of CRC by 70% [4]. Another important risk factor to consider is obesity, often associated with hyperinsulinemia and insulin resistance, major causes of the free insulin-like growth factor 1 (IGF1) increment. The insulin/IGF1 pathway stimulates the evolution of the pathology by increasing cell proliferation and decreasing apoptosis [4].

CRC is generally an asymptomatic disease until it progresses to an advanced stage over the course of 5-10 years [1], and it can arise both on the right (ascendent) and the left (descendant) side of colon[5]. The different embryologic origins of the two side of colon, according to many studies, impact on the biological features of cancers and consequently on the patient survival and treatments response [6]. Tumours that arise on right colon, which originates with the midgut and derives its blood supply from the superior mesenteric artery, are mostly associated with fatigue, abdominal pain, cramping and anemia [5], [6]. Regarding to left colon, that during embryogenesis develops with the hindgut and is supplied by the inferior mesenteric artery, patients with left-sided CRC suffer from constipation, rectal bleeding or narrow caliber stool [5], [6]. Independently from the anatomical site where it develops, CRC is caused by the accumulation of different genetic and epigenetic mutations that lead to the activation of various pathophysiological mechanisms linked to oncogenesis such as abnormalities in cell proliferation and differentiation, resistance to apoptosis, invasion of adjacent tissues and of course metastasis [3], [4]. According to the origin of the mutations, CRC can be categorised as sporadic, familial and inherited. Most of CRCs are sporadic with no family history, and are also associated to adenoma-carcinomas, tumours originated from the malignant degeneration of adenomas [4], as shown in Figure [2]. In these cases, the normal colorectal epithelium is transformed into benign adenomatous polyp through the adenomatous polyposis coli (APC) mutations [4]. Approximately 10% of adenomatous polyps evolve to adenoma-carcinoma[3] through transformation processes, illustrated in Figure [2], causes by three major pathways of genome instability [4]:

- Chromosomal instability (CIN)
- Instability of microsatellite DNA regions (MSI)
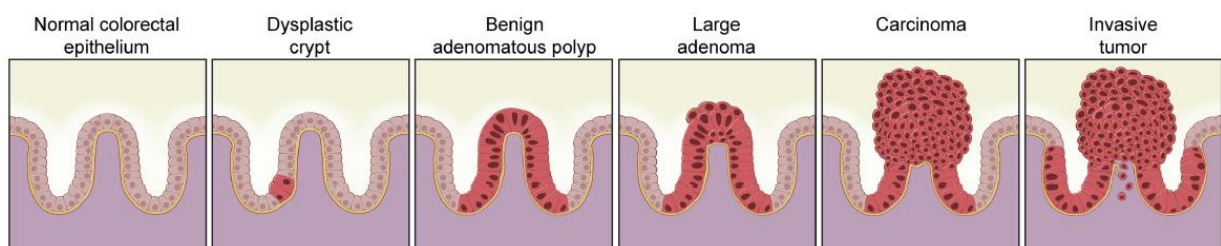- Methylation of CpG island methylator phenotype (CIMP)

Figure 2: Representation of adenoma-carcinoma development [7].

Although the disease is mainly sporadic, about 30% of patients with CRC have a family history and one third of them develop the illness during their lifetime [3], [4]. For those who have a family history in a first-degree relative, the probability to contract the pathology is 2 to 4 higher than in general population [3]. In 5-10% of cases instead [4], the disease is caused by inherited gene mutations that lead to genetic syndromes such as *Lynch syndrome* and *Familial adenomatous polyposis* (FAP). The first one, which is associated to MSI, is the most common inherited colorectal syndrome and is characterised by low presence of adenomas. On the contrary, patients with FAP are more prone to develop adenomas especially under the age of 40 [4].
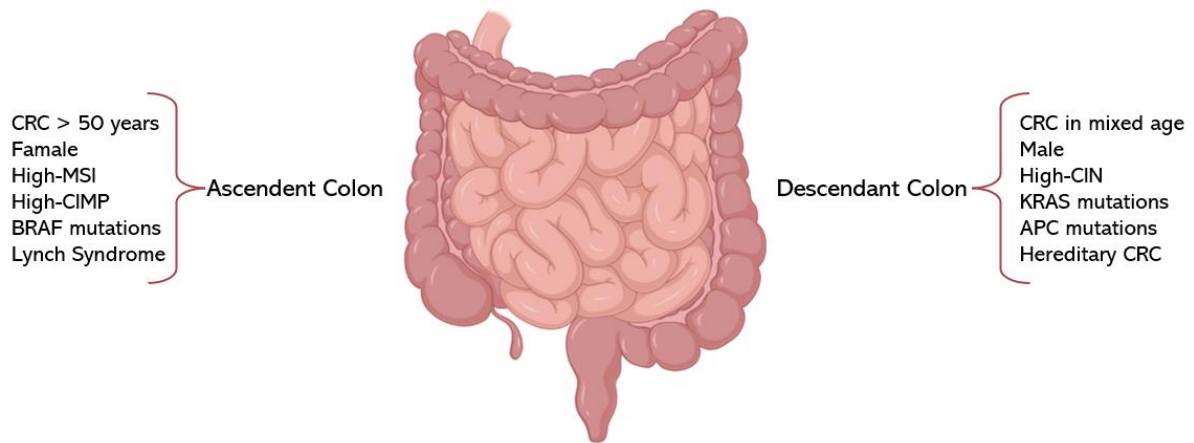
Figure 3: Schematic association of CRC collocation and genetical, sex and age factors.

The development of CRC is structured into four distinct phases, according to which the pathology can be classified as early-stages (I-II) or late-stages (III-IV). The first step of this process is known as *Initiation*, which consists of all the genetic alterations that lead to the neoplastic transformation. The next phase, namely *Promotion*, is associated to hyper cell proliferation which causes abnormal cell growth, followed by the translation from benign cells to malignant ones during *Progression* stage. The last phase is called *Metastasis* and consists in the tumour's ability to spread out to other organs through blood and lymphatic vessels, acquiring more aggressive characteristics [4]. Metastasis represents the primary cause of CRC deaths [8], in fact it turned out that 20% of patients have metastatic disease at the time of the diagnosis while 25% of them will develop metastasis during the progression of the disease itself [9].

1.2. Metastatic colorectal cancer

Metastatic CRC (mCRC) can be defined as a set of tumours that grow at a distant site from the original colorectal mass mainly at lymph nodes, liver, lungs, and peritoneum [5]. Less frequently, CRC can metastasise to other organs as brain, bones, or adrenal glands according to several factors which play crucial roles in metastatic organotropism, namely the inclination of metastasis to target specific organs [8]. Regardless the target organ, the process occurs through the dissemination of primary cancer cells via blood or lymphatic vessels until they reach the metastatic site. The tendency of mCRC cells to colonise specific organs is associated to many aspects as the organ-specific microenvironment, the layout of the circulatory system, the immune response, the metabolic reprogramming mechanisms, but also tumour-related genes, nanosized vesicles (30-150nm) called tumour-derived exosomes (TDEs), and of course intrinsic properties of cancer itself [8].
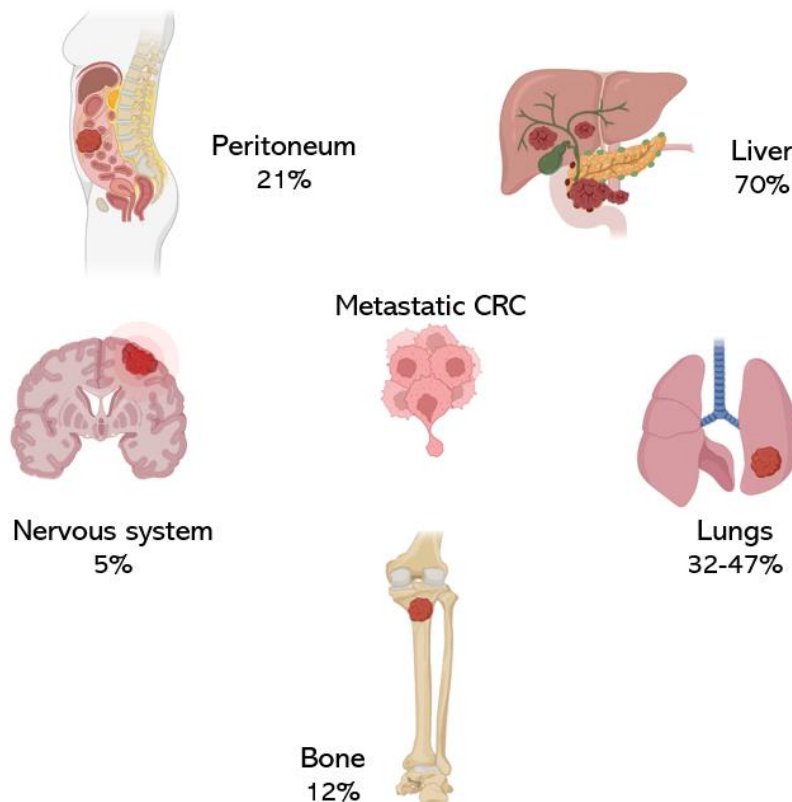
Figure 4: Principle metastatic site of CRC and their frequency according to [10].

A key aspect of the metastatic process is the capability of mCRC cells to adapt to environmental conditions which are different from the native ones. To correctly colonize other organs in fact, mCRC cells undergo metabolic reprogramming that consist of changes in glucose, lipids, and amino-acids metabolism. This strategy ensures both cancer cells' high-energy necessity, associated with hyper proliferation, and their survival through bloodstream or lymphatic system transport [8].

Metastasis begins with the secretion, by primary tumour cells, of TDEs which contain different biomolecules as DNA, RNA, human biofluids, but also lipids, proteins and glycans. These extracellular vesicles can interact with integrin patterns of the target and organ-specific cells to establish pre-metastatic niches (PMNs). TDEs are also able to modulate local cells within the PMNs through numerous signalling pathways, allowing the reorganization of the secondary site to enable successful tumour colonization. Moreover, TDEs are involved in many other mechanisms associated with tumour dissemination such as the regulation of immune response, the improvement of angiogenesis process and the promotion of epithelial-mesenchymal transition (EMT) [8], shown in Figure 5.
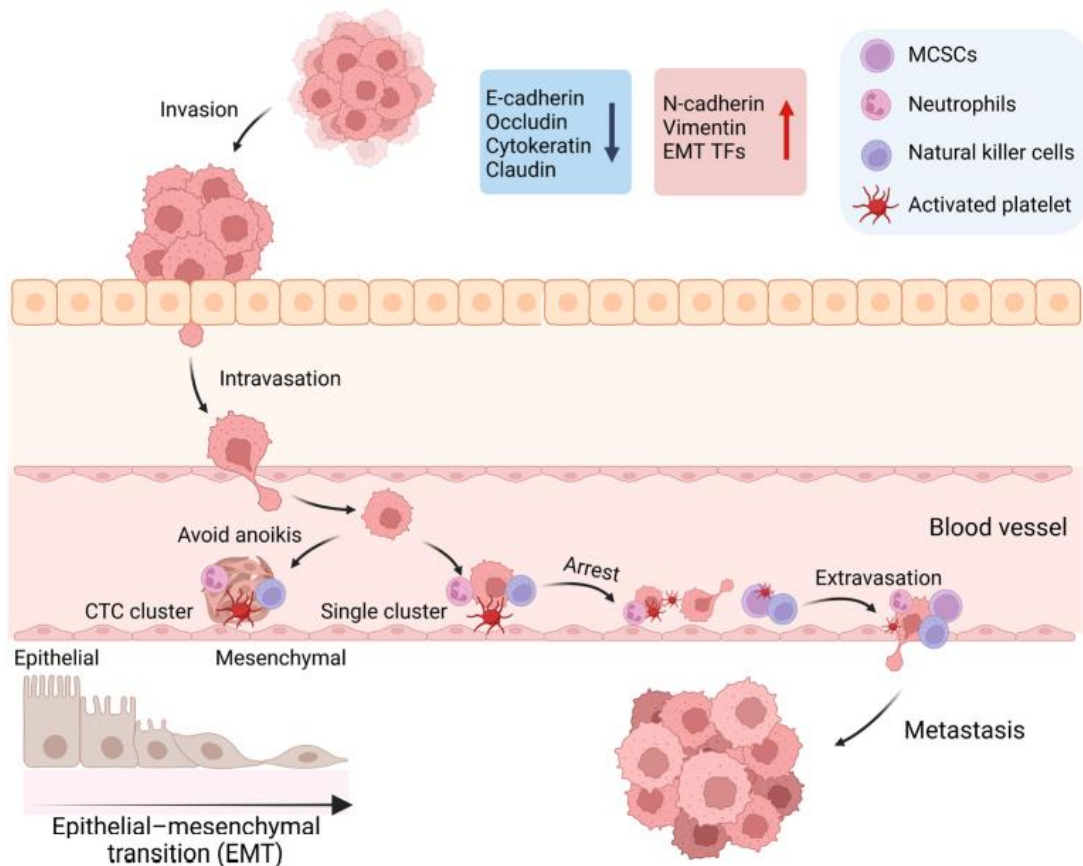
Figure 5: Schematic illustration of EMT pivotal role in mCRC [8].

EMT is a phenome by which epithelial cells undergo changes that allow the loss of intracellular adhesions, promoting their detachment from the primary tumour. This process allows the escape of cancer cells from the basement membrane which surrounds the tumour, through phenotype transformation of the in-situ tumour cells. Once EMT cells reach the metastatic site, metastatic cancer stem cells (MCSCs) breach the endothelial barrier, infiltrate the mesenchymal stroma and spread into neighbouring tissues through the blood streaming or lymphatic system. To elude

immune surveillance and promote their survival, circulating tumour cells interact with platelet coagulation factors and neutrophils [8].

Prognosis for mCRC patients depends on the molecular profile of the primary tumour but generally the survival at 1, 3, 5 years is about 70-75%, 30-35% and 20%, respectively [9]. According to the consensus molecular subtype (CMS), mCRC can be classified into 4 different groups [3]:

- **CMS1**, associated with MSI and active immune response;
- **CMS2**, related to the activation of specific signalling pathways (Wingless/Integrated (WNT) or Myelocytomatosis (MYC));
- **CMS3**, referred to metabolic dysregulation and higher activity in glutaminolysis and lipidogenesis;
- **CMS4**, correlated to EMT and immunosuppression.

MSI affects about 5% of mCRC patients [5] and it occurs because of the accumulation of numerous insertions or deletions at site of repetitive DNA units called microsatellites. These replication errors are generally correct through the proteins of the mismatch repair (MMR) system but when mismatch repair deficiency (MMR-D) is present, these repairs are not performed [5], [9]. According to the comparison of specific biological markers between healthy and pathologic tissues, patients with MSI are typically divided into three different classes: MIS-high (MSI-H), MSI-low (MSI-L) and MSI-stable (MSS) [9].

Approximately 35-45% of mCRC cases are instead correlated to Rat sarcoma virus oncogene (RAS) sequence mutations [5]. Normally, these genes are involved in the Epidermal Growth Factor receptor (EGFR) signalling pathway which is responsible for the increase of cell proliferation, survival, migration, and invasion through the activation of mitogen-activated protein kinase (MAPK) pathway [2]. In presence of mutations, the proteins synthetized by RAS genes are constitutively triggered promoting cell hyperproliferation and leading to tumorigenesis [2]. One of the most common mutated proto-oncogenes is Kirsten rat sarcoma (KRAS) often associated to distant metastasis, lack of tumour differentiation, poor survival and the necessity of targeted and personalized therapies [11].

In addition to RAS mutations, mCRC tumours can be also associated to B-Raf proto-oncogene (BRAF) variants which affect about 5-10% of patients[2], [5]. Normally, BRAF gene encodes a protein kinase in the MAPK pathway, which is directly activated in response to signals from receptor tyrosine kinase through RAS family members[9], [12]. BRAF mutations are responsible both for cell hyperproliferation and apoptosis inhibition due to the RAS-independent activation of MAPK pathway and BRAF kinase, via downstream activation of mitogen-activated extracellular signal-related kinase (MEK)[12].According to many studies, these mutations are prevalent in old

patient, especially women, with right-side and poorly differentiated tumours [5]. They usually originate from serrated adenomas characterised by low rates of CIN and MSI-H and are mostly correlated to peritoneal and lymph nodes metastasis. Standard treatments for this kind of patients are not very effective [13].

Patients with KRAS/BRAF wild-free mCRC have instead better prognosis than those with genes sequence variations and represents about 50% of cases. The median survival is approximately 30 months with treatment and the survival rate is about 80% at 1 year, 40% at 3 years and 20% at 5 years after first-line therapy [5].

Finally, about 2-5% of mCRC presents amplified human epidermal growth factor receptor 2 (ERBB2), which promotes the development of different cancer types, including CRC. ERBB2 is a tyrosine kinase receptor that normally is implicated in cell processes such as growth and differentiation but in mCRC is associated with cancer aggressiveness. For patients with this molecular subtype, targeted therapies are required [5].

1.2.1. Clinical approved therapies for mCRC

Many therapies are nowadays available for mCRC, for example specific surgical techniques if the primary tumour and all the metastases can be totally removed. These approaches cannot be applied for patients with unresectable tumours or surgical intolerances [2]. Therapeutic strategies are strongly dependent on the tumour type, and in the majority of cases, a combination of treatments is necessary. Figure 6 shows the main therapies option according to mutational profiles, as well as the median overall survival time for patients that are healthy enough to undergo intensive treatments.
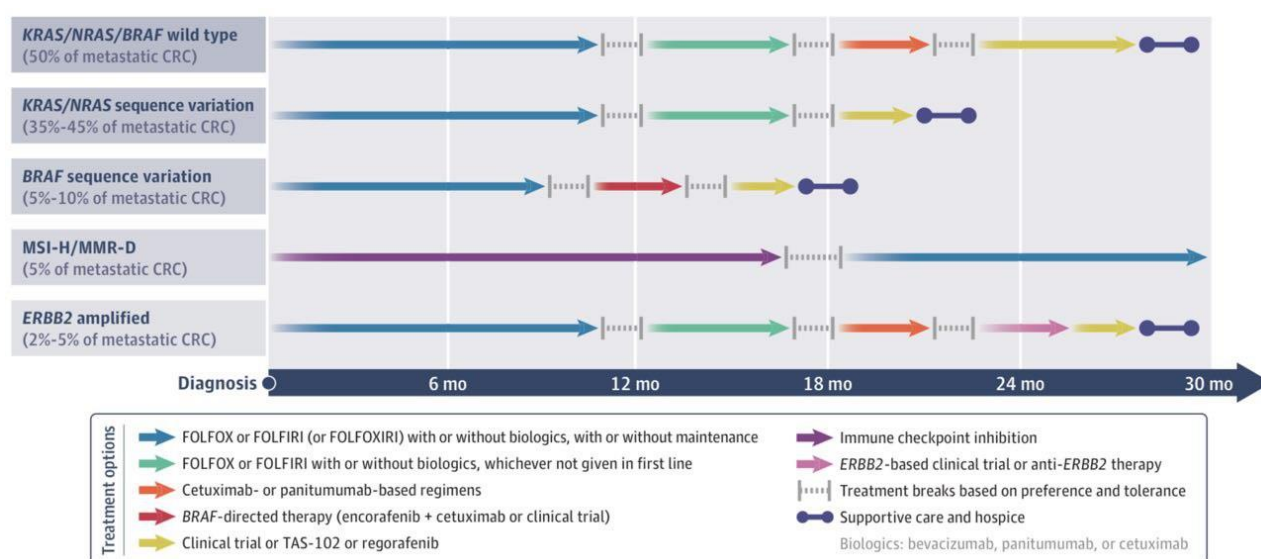
Figure 6: Prototypical treatment for patients with unreseactable mCRC according to molecular subtype [5].

To reduce the size and slow down the tumour growth, chemotherapy represents one of the most effective methods and it can be used as neoadjuvant or adjuvant treatment before or after surgery [2]. First-line therapy for mCRC patients usually consists in the intravenous administration of *fluorouracil* or in the oral administration of *capecitabine*, which are pyrimidine antagonists or antimetabolites able to tamper DNA synthesis [5]. These chemotherapeutic agents are combined with other drugs so that this kind of therapy is divided into: oxaliplatin-based regimens (FOLFOX or CAPOX) and irinotecan-based regimens (FOLFIRI or CAPIRI) [3]. Several studies have shown that the use of these regimens as first-line therapies for mCRC result in similar overall survival such that, in some cases, both treatments are applied for the same patient [5].

Unfortunately, chemotherapy is not always the most effective therapy to adopt. For example, MSI-H patients tend to respond less to conventional chemotherapies despite their better prognosis. In these cases, the currently approved treatments are three different regimes of immunotherapy: *Pembrolizumab*, *Nivolumab* and, the combination of the latter with *Ipilimumab* [9]. These approaches present however side effects associated with toxicities, due to the inhibition of immune

system's normal protection from immune overactivation, but also hepatitis, thyroiditis, pneumonitis, colitis, and dermatitis [5].

Patient survival is closely related to the tumour's molecular subtype, which is why chemotherapy is often combined with *targeted* therapy, namely the administration of certain drugs able to target specific biological features instead of directly kill tumour cells [2], [5]. In this perspective, the detection of the molecular type plays a crucial role in the identification of the correct treatment. For all mCRC patients it is possible to carry out a molecular tumour profiling, that consists in a pathologic test of tumour tissues able to find MSI or MMR-D, but also variations in RAS/BRAF genes [5].

The principles mCRC targeted therapies approved by the United States Food and Drug Administration (USFDA) today are:

- EGFR targeted therapy;
- Targeting vascular endothelial growth factor (VEGF) therapy;
- DNA therapy [2].

The EGFR targeted therapy is a treatment used for patients with EGFR overexpression, that occurs from 25 to 82% of CRC cases, and associated with cancer progression, reduced survival and poorly differentiated tumours [9]. EGFR is a tyrosine kinase receptor involved in the regulation of different biological mechanisms such as cell growth, proliferation, migration, differentiation and apoptosis. Binding to specific ligands, EGFR undergoes self-phosphorylation by which occurs the activation of transcriptional factors necessary for all the processes mentioned above [9].

The EGFR targeted therapy focuses on the use of EGFR inhibitors namely *Cetuximab*, a chimeric (mouse/human) immunoglobulin antibody, and *Panitumumab*, a humanized monoclonal antibody, which are generally interchangeable [2], [5]. Several studies have shown how the combination of such inhibitors with other chemotherapy regimens can increase the median overall survival [2]. Despite its efficacy, this treatment results useless for patients with RAS genes mutations that determine the constitutively activation of RAS proteins which brings to an uncontrolled and independent cell growth from the ligand-EGFR interaction [9]. Patients with these mutations in fact tend to develop more aggressive cancers, refractory diseases, and unfortunately there are still no approved therapies able to increase their survival by 3 or more months [5], [9]. Those who present RAS wild-type tumours instead, have usually better prognosis because they correctly respond to EGFR targeted therapy [5], [9].

EGFR inhibitors are also used in combination with BRAF inhibitors as *Vemurafenib* or *Dabrafenib*, for BRAF-mutated mCRC that are usually characterized by overactivated EGFR pathway. Due to the low effectiveness of BRAF inhibitors monotherapy, many studies have

investigated the potential of these combinations, revealing that the Panitumumab and Dabrafenib combination increase patient response from 5%, response rate yielded by BRAF targeted monotherapy, to 10% [9], [12]. Moreover, some trials demonstrate that BRAF inhibitors lead to raised progression-free survival (PFS) from 2.5 to 3.5 months respect to traditional chemotherapies, if used in combination with *Trametinib* [13]. Trametinib is a targeting agent which is able to inhibit MEK pathway, downstream of BRAF in the MAPK pathway, in all cells but, at the same time, it is responsible for a high systemic toxicity [12], [13]. For this reason, the dose of Trametinib, that must be limited to ensure patients health, turns out to be suboptimal for the correct MAPK inhibition [12]. The greatest degree of MAPK inhibition is achieved by the combination of BRAF, EGFR and MEK inhibitors, that leads to a response rate around 21%, assuring the inhibition of both the dependent and independent activation of this signalling pathway [12]

Another targeted therapy is represented by VEGF therapy, commonly applied for mCRC patients with upregulation of VEGF signalling that promotes angiogenesis and subsequent cell proliferation. Angiogenesis is used by most of solid tumours to fulfil their need of high blood supply and consequently high nutrient intake to stimulate tumour growth. The VEGF pathway embodies therefore a potential target that can be blocked to prevent angiogenesis by many drugs [6]. The first VEGF therapy approved by USFDA consists in the administration of *Bevacizumab*, a humanized monoclonal antibody able to bind to the VEGF receptor, which is often added to chemotherapy regimens such as FOLFOX4. It has been shown that, respect to the use of Bevacizumab alone, these combinations enhance the patient overall and PFS but are not recommended as adjuvant therapies after surgery. Other strategies able to improve the survival of patients based on anti-angiogenesis agents are *Aflibercept* or *Ramucirumab* combined with FOLFIRI, but also *Regorafenib* and *Fruquitinib* that are mostly administered for all patients who have previously failed other treatments [6].

The development of novel cancer therapies is a complex and challenging process which generally requires the creation of appropriate models able to mimic in a realistic way the pathologies. One of the principal problems is the frequent failures, during clinical trials, of drugs that demonstrate efficacy in *in vitro* models. Two-dimensional (2D) approaches in fact, present many limitations related for example to the inability to reproduce the typical three-dimensionality of in vivo tissues, affecting not only cell-cell and cell-extracellular matrix (ECM) components interactions, but also cell morphology, the expression of genes, proteins, biomarkers and therefore drug response[14].

Over the years, alternative strategies based on three-dimensional (3D) *in vitro* approaches have been developed both to provide solutions to most of the problems of traditional methods and to increase the models' complexity through the introduction of all the other components of the tumour

microenvironment (TME). TME is in fact characterized not only by cancer cells, but it is also composted of ECM, vasculature network, and different cell types such as tumour-infiltrating immune cells, mesenchymal stomal cells and tumour-associated macrophages, shown in Figure 7. Each of these cellular populations represent disease-defining factors, able to interact with cancer cells and drive all the early and late stages of the pathology progression, as well as therapeutic response, by supporting processes like tumour cells proliferation and angiogenesis. Accurately replication of cancer heterogeneity and its interaction with TME components, together with the ability to reproduce ECM stiffness comparable to that of the in vivo environment, is essential for 3D models to preserve the phenotypic and genotypic characteristics of original tumours, making them valuable tools for personalized medicine[14] .
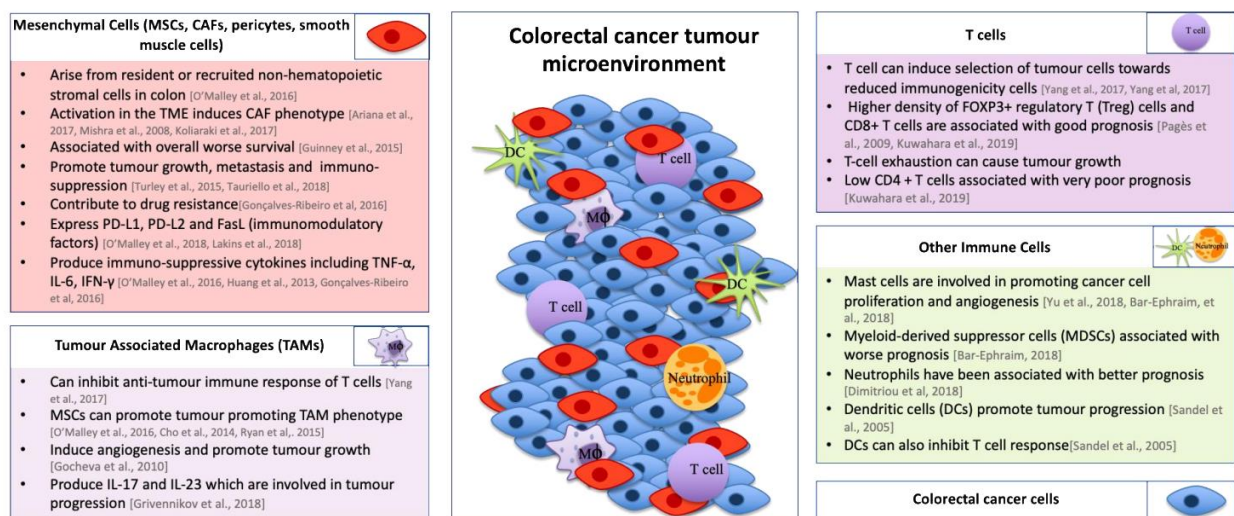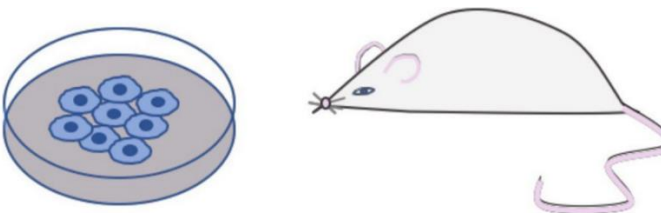

Figure 7: Description of TME components of CRC and short description of their role in tumour progression[14].

1.3. 3D Models Systems for Colorectal Cancer

Cancer research was focused for many years on the use of in vitro 2D monolayer cell cultures and in vivo xenografts or animal models as screening methods to investigate cancer biology and to evaluate the safety and the potential of different drugs [15]. Despite the numerous advantages of all these systems, especially associated to the high reproducibility and standardization at low costs, there are still many drawbacks which led to the development of new methodologies. In particular, 2D models do not recreate the 3D tissue-tumour architecture and even in case of co-culture systems, are not able to reproduce the intra-tumour heterogeneity and the dynamic interactions between cancer cells and TME components [15]. When cultivated on plastic layers moreover, cells respond differently to treatments respect to 3D cultures due to the alterations in intracellular signalling and gene expressions, both consequences of bidimensional culture [14]. Regarding to animal models, the main limitations are related not only to ethical problems but also to the differences in genetic characteristics, immune contextures and growth environments that can influence the therapeutic response [15]. The major advantages and limitations of these models are presented in Figure 8.

	2D cell culture	In-vivo model
Advantages	• Low Cost • Ease of use • Highly reproducible • Can be used for high-throughput drug screening	• Living organism • Heterogeneity present
Disadvantages	• Not representative of in-vivo interactions • No TME/ECM • Often not clinically relevant	• Not human • High Cost • Require skilled individuals • Ethical limitations • Large scale experiments not possible

Figure 8: Summary table of the main advantages and disadvantages of traditional cancer models [14].

Nowadays, 3D models represent the most employed to study cancer progression and drug efficacy, due to their faithful reproduction of TME which results to be essential for the correct prediction of therapeutic response. The first 3D models of CRC emerged in the early 1900s, marking the start of a progressive evolution that still continues today. The most significative discoveries that led to the development of cutting-edge models currently used, are illustrated in Figure 9 [14] .
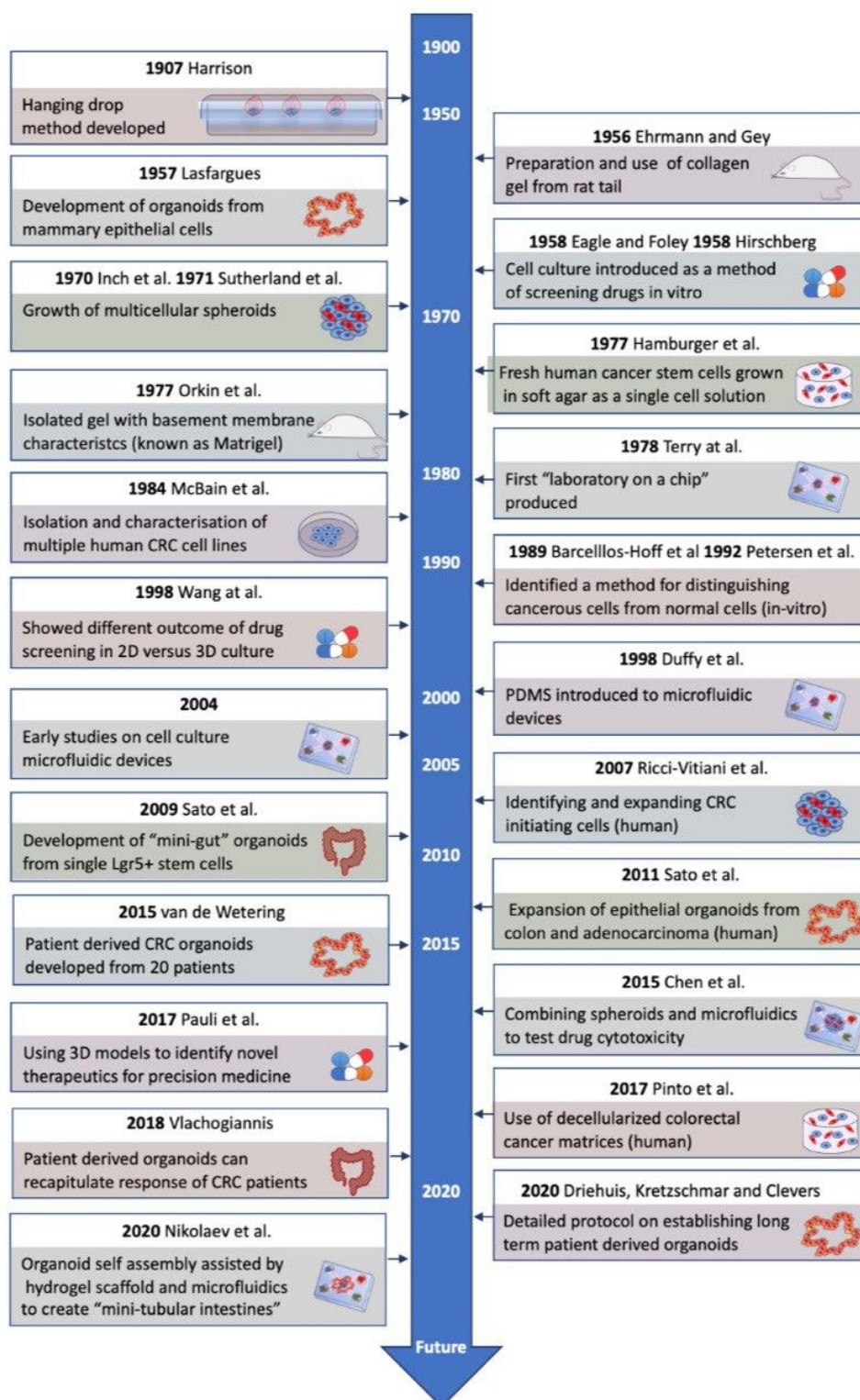
Figure 9: Historical overview of 3D model development in CRC research [14].

13

Nevertheless, these systems still present many challenges, for example maintaining stable and reproducible cultures because of cell batches variability and the occasional use of specific devices, as microfluidic channels or bioreactors, to provide mechanical/biological stimuli but also controllable parameters as pH, temperature and oxygen. In particular, oxygen distribution is one of the main shared criticalities by most of 3D models, due to diffusion barriers presence (i.e., ECM-resembling matrices) and because of the systems' morphological structure (i.e., organoids, spheroids), both aspects which lead to the development of oxygen gradients. While cells located in peripheral regions receive adequate oxygen supply, the ones sited in the internal areas suffer of oxygen deficiency, main cause of hypoxia. This dysfunctional condition brings to many consequences as decreased cell proliferation, alterations in metabolic pathways and impaired gene expression, all changes that are associated with the development of drug resistance. Moreover, the evaluation of therapeutic response in 3D models results more difficult than in 2D systems due to the lack of standardized protocols. Finally, another drawback consists in the correct cells isolation from 3D constructs without affecting their functional and structural integrity [16]. Regarding to mCRC studies, the principal 3D approaches include tumour-derived organoids, conventional and unconventional matrices able to replicate ECM environment.

1.3.1. Tumour-derived organoids

Developed for the first time in the early 2000's, organoids are 3D self-organized and self-renew models, derived from human stem cells and able to reproduce cellular variety, structural and functional organization but also genetic signature of normal and tumour tissues[15]. They can be defined as mini clusters of cells that start to self-organized through the activation of many signalling pathways and differentiate into functional cell types [17].

The ability to replicate physiological and pathological 3D architecture, together with the possibility of long-term cultures, make organoids one of the most versatile tools in multiple biomedical applications, as illustrated in Figure 10, ranging from disease *in-vitro* modelling to regenerative medicine and gene editing studies [17].
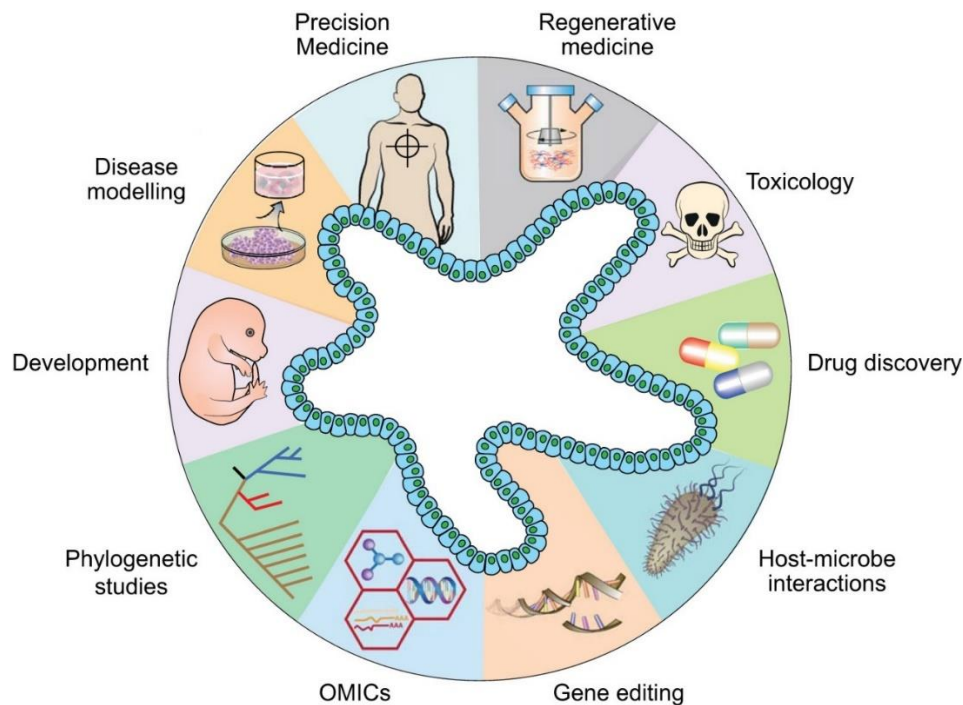
Figure 10: Representation of principal organoids' application areas [17].

According to the type of stem cell from which organoids derived, there are three different groups where they are classified: embryonic stem cells (ESCs)-derived, induced pluripotent stem cells (iPSCs)-derived and adult stem cells (ASCs)-derived. ESCs and iPSCs can generate organoids from each of the three germ layers through the use of many growth factors or inhibitors while ASCs-derived organoids are developed from postnatal or adult tissues and in case of tumour-derived organoids (TDO) they are generated directly from patient tissues [17].

The organoids generation includes suspension culture, which is required to prevent the direct interaction between cells and plastic layers and is based on the use of scaffolds or free-scaffolds

approaches. Scaffolds are natural or semi-synthetic matrices resembling the environment of native tissues, not only due to the presence of ECM components but also because they supply the same structural support [17]. Generally, organoids are embedded in drops of a naturally derived matrix called Matrigel (Corning) that, in some cases, is also used as basal layer for cell culture. This layer is covered by medium that evaporating, leaves cells exposed to the air, allowing their polarization and differentiation[17].
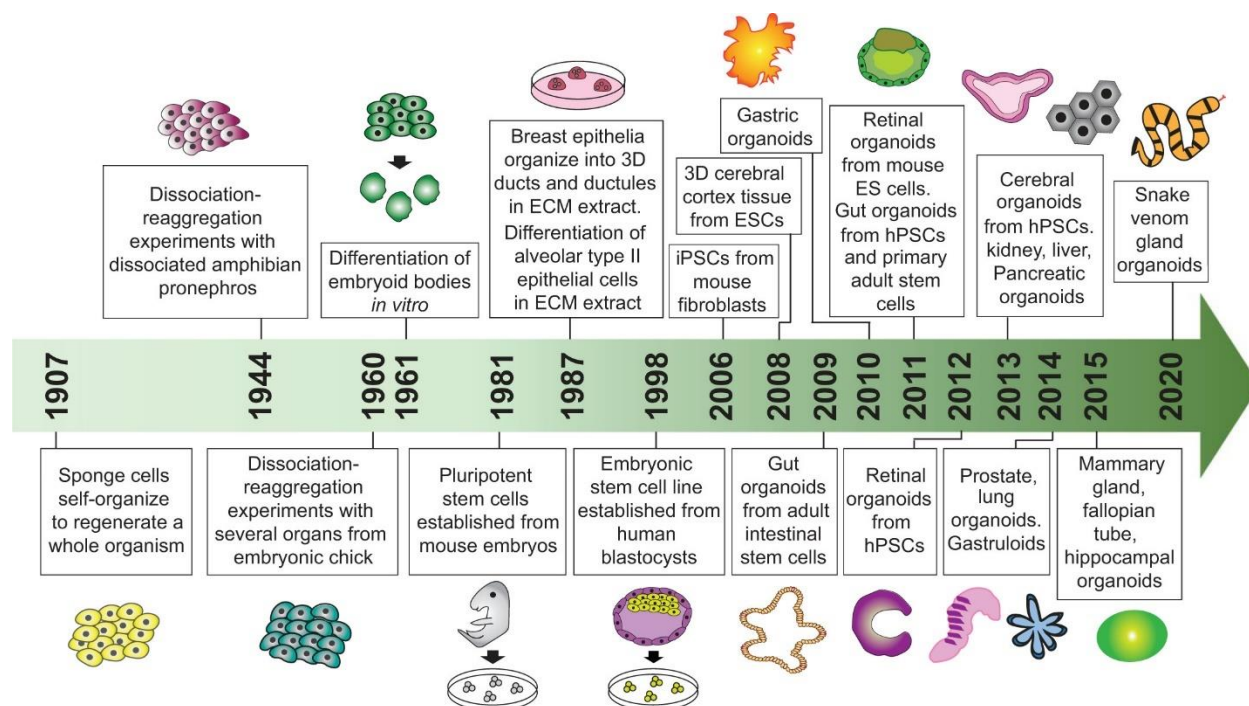
Figure 11: Schematic overview of pivotal studies that lead to the development of organoid technologies [17].

Regarding to TDO, they represent a viable alternative to conventional models employed in oncology research, allowing a deeper understanding of disease onset and progression, and therefore contributing to the improvement of clinical treatments in the long term. In fact, TDO maintain not only the genetical, mutational and morphological characteristics of the original tumours, but also all the pathological transformations, offering a promising platform for the personalized therapy which is based on the genetic, environmental and lifestyle characteristics of each patient. Moreover, TDO are used as drug screening methods to investigate the sensitivity of patients to chemotherapeutic agents and as preclinical models to evaluate the toxicity and thus the safety of drugs [1].

The first organoid of colon adenocarcinoma was developed by *Sato et al.* [1], through the expansion over long periods of single crypts or stem cells derived from mouse small intestine. This process results in the formation of the typical villus-like epithelial domains, illustrated in Figure 12, characterized by all the differentiated cell lineages (colonocytes, goblet cells, enteroendocrine

cells, Paneth cells) after multiple crypt fission events [18], [19]. Culture conditions were subsequently tailored to generate epithelial organoids from mouse and human colon, and human small intestine [19]. Unfortunately, even nowadays there are no standardized methods for the culture of CRC organoids whether they are obtained from surgical resections of primary tumours or generated through the introduction of specific mutations into organoids derived from normal intestinal epithelial cells [1], [15].
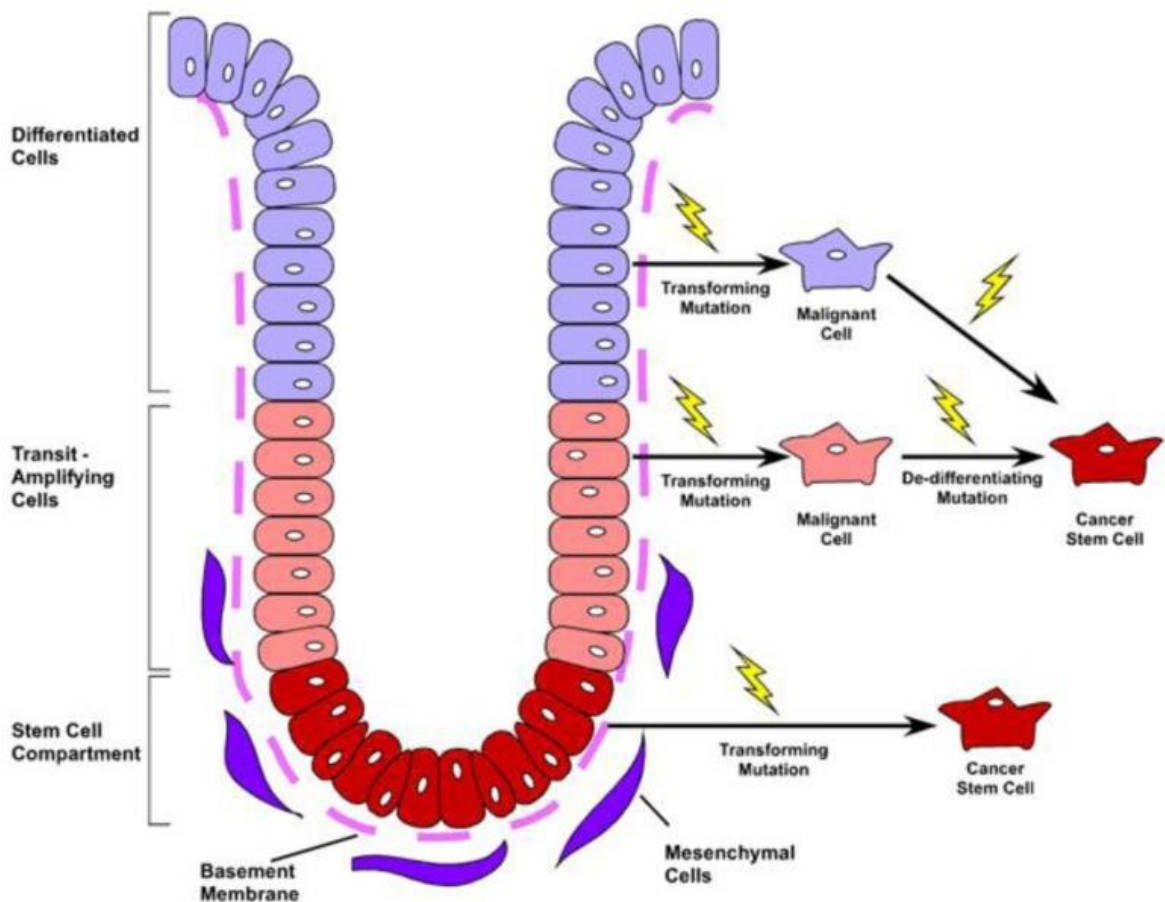
Figure 12: Schematic representation of human colonic crypt structure and mutations that lead to the development of cancer stem cells [19].

Nevertheless, CRC organoids, that are shown in Figure 13, result to be simple to set up and inexpensive to manage, providing many high throughput strategies for precision medicine also due to their 90% similarity in somatic mutations with original tumours [14], [15]. According to some studies in fact, the correlation of DNA copy number profiles between these organoids and patient samples is about 0.89, proving once again how they are best suited to model the pathology in all its phases [14]. Beyond cancer modelling, they represent a viable platform for basic cancer research to investigate the cellular and molecular processes that characterize the disease progression [20]. One of the main advantages of CRC organoids is therefore the possibility to reproduce the complex relationship between cell polarity and tissue changes that occur during the development of CRC [1]. Moreover, the maintenance of the genomic heterogeneity, together with the possibility of cryopreservation and the genetic stability up to 6 months, make them powerful tools for anticancer therapies [1], [20].
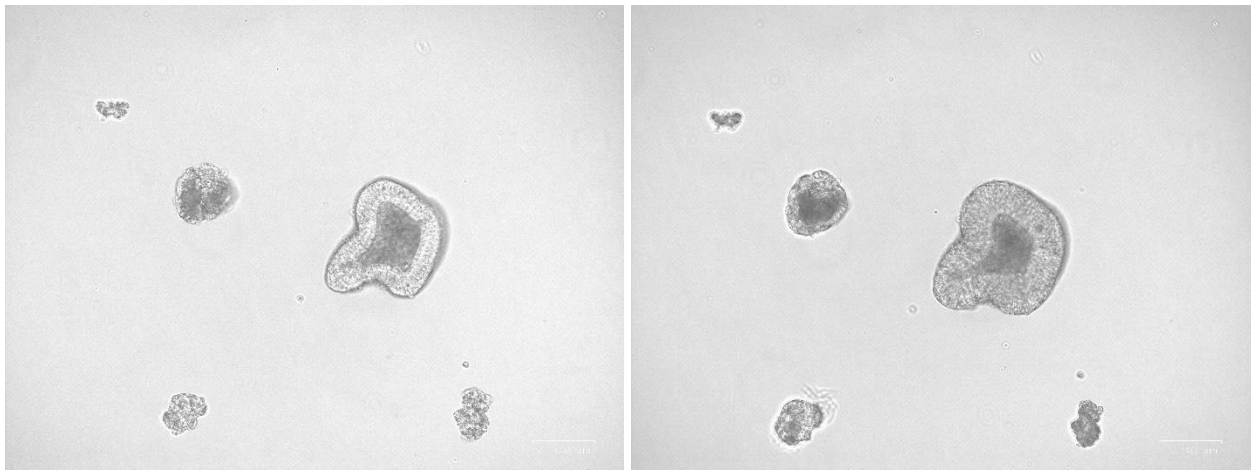
Figure 13: Brightfield microscopy images showing time evolution (day1-day3) and organization of mCRC organoids. (Scale bar: 100 μm)

Although CRC organoids provide substantial benefits and achieve a success rate formation approximately of 70% [15], this technology requires further optimizations from multiple perspectives. One of the most critical challenges in organoids generation is the limited number of cancer cells typically available from biopsy specimens. This limitation is more evident in case of rare CRC histological subtypes, for which the creation of organoids results to be more difficult. Moreover, the exclusive presence of tumour epithelium in CRC organoids, do not recreate the heterogeneity of the TME that impacts on the development and treatment response of the pathology [1].

1.3.2. Conventional 3D Matrices

The use of 3D matrices as culture methods able to provide 3D environments like native ECMs, is an essential requirement for the correct growth, differentiation and organization of cells and therefore organoids. The most widely used in biomedical fields is Matrigel, a complex matrix derived from the secretion of Engelbreth-Holm-Swarm mouse sarcoma cells, that at 37°C can polymerise to form a bioactive 3D matrix [21], [22]. Described for the first time in the mid-1980s, Matrigel has been extensively employed as supportive substrate for 3D cell cultures and in vivo applications to study cellular differentiation, tissue development, pathological mechanisms and to evaluate the activity of pathway modulators, drug screening and toxicity [23].
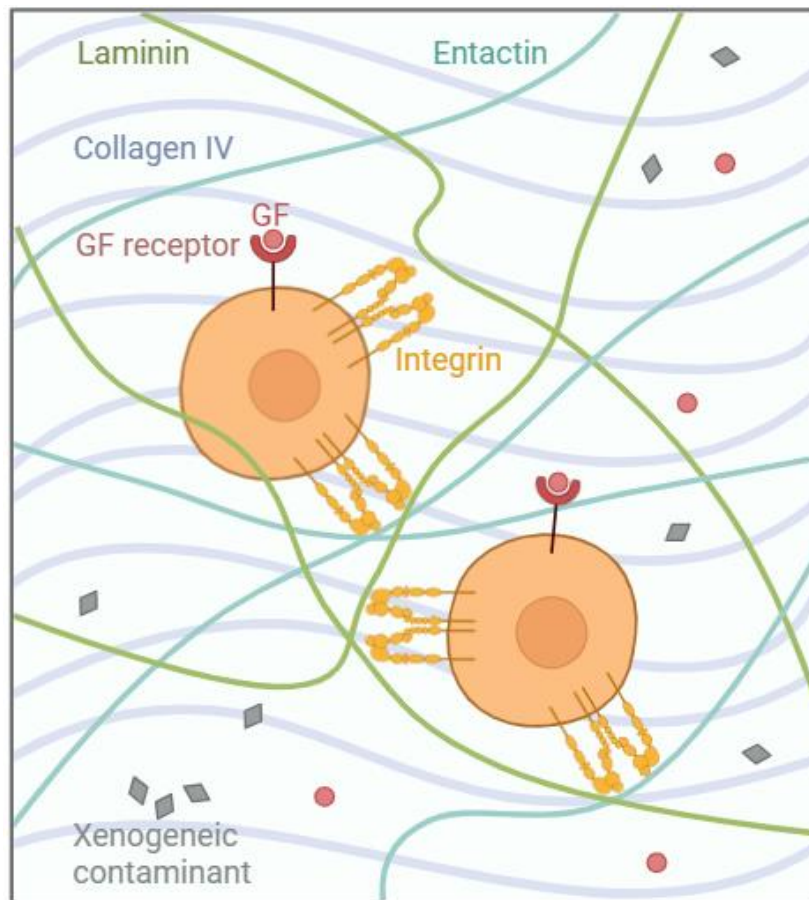
Figure 14: Illustration of main Matrigel's components

According to proteomic analysis, Matrigel contains more than 1800 unique proteins which make the material extremely heterogenous so that it becomes very difficult both to control the culture conditions and to detect signals implicated in cellular developments [24]. Nevertheless, nowadays Matrigel is still considered the gold standard in cellular biology due to its bioactivity, mostly related to the presence of many soluble growth factors, that promotes the differentiation of multiple cell types and the self-organization of complex structures [25]. As shown in Figure 14, in addition to growth factors, which are in this case tumour-derived, Matrigel is rich in other ECM components

as: laminin, that represents about 60% and is responsible not only for the attachment of different cell types (stem, endothelial, epithelial and tumour cells) but also for the promotion of differentiation and angiogenesis processes; collagen, especially type IV, that constitutes 30% of the matrix; entactin and heparin sulphate which are respectively the 8% and 2-3%. During polymerization, laminin and collagen IV are responsible for the generation of the 3D matrix thanks to the presence of entactin that serves as crosslinker agent [26].

Matrigel offers many advantages related to its high availability, remarkable versatility and practicality of being provided as a ready-to-use product. In addition, the realisation process results to be relatively easy and consists in repeated saline extractions/washes of the tumour homogenate to remove all the soluble proteins while the insoluble components are delated by chaotropic agents. The final solution is obtained after centrifugation and dialysis versus tris buffered saline at pH 7.4 in the cold [23]. This material can be employed in many ways depending on the users' needs, for example thin Matrigel coatings allow cells culture and expansion, thicker coatings are instead used as assays especially for the investigation of endothelial tubulogenesis, while 3D Matrigel matrices enable cells encapsulation and organoid assembly [26]. Regarding to the use of Matrigel as 3D matrix for organoid cultures, several studies have demonstrated that also for CRC organoids, this matrix effectively support cell proliferation, preserving the organo-specific morphology and allowing long-term cultivations [27], [28].

Research is currently focused on the development of Matrigel alternatives due to its multiple criticalities which are largely linked to its animal derivation. One of the major risks in fact is the transmission of animal pathogens and viral or xenogeneic contaminants, such as lactate dehydrogenase-elevating virus, a normal mouse virus that can influence tumour behaviour and affect immune system [26]. The activation and expansion of T lymphocytes in immunological models based on human cells in fact, is quite frequent due to mouse proteins [21]. Moreover, the unknown composition together with the presence of growth factors in an undefined quantity, are crucial factors that contribute to the batch-to-batch variability, limiting experimental standardization and reproducibility [21]. This variability also results in significant differences in mechanical properties, especially in terms of Young Modulus that shows higher or lower values according to the analysed region [26]. In contrast to other materials, Matrigel exhibits very limited mechanical tunability, making it less suitable for all the applications that require defined physical characteristics such as in organoids culture. Considering the unique ECM of different tissues, parameters like the substrate stiffness play pivotal role in faithfully reproducing the main characteristics of the native in vivo setting which influence cancer hallmarks. It is also essential to provide a tissue-specific environment in terms of composition to promote the development and

maturation of organoids; therefore, the presence of undefined growth factors should be minimised. Other disadvantages are associated with ethical issues as well as high production costs and difficulties in handling it without the use of ice [21], [29]. The main limitations of Matrigel can be overcome through new engineered materials as natural or semi-synthetic hydrogels that are optimized to fully replicate ECM profile.

1.3.3. Hydrogels

Hydrogels are highly hydrated matrices of cross-linked polymers widely used in biomedical fields to mimic the native ECM by providing 3D environments suitable for cell growth[30]. Due to their ability to absorb huge quantity of water (water content >90%) and thanks to their structure and porosity in fact, hydrogels closely resemble living tissues and are therefore employed in tissue engineering to support the regeneration of tissues as cardiac, cartilage, bone, and nerves but also in wound dressings [31]. In this perspective, hydrogels are also employed as 3D models of different illness like tumours, inflammatory bowel diseases, tissue fibrosis, nerve diseases etc in order to investigate the pathogenesis and contribute to the development of new therapies [32]. Drug delivery represents another biomedical application of these matrices which in this case are able to respond to specific stimuli, as pH variations, enabling controlled drug kinetics through non-intravenous administration[31].
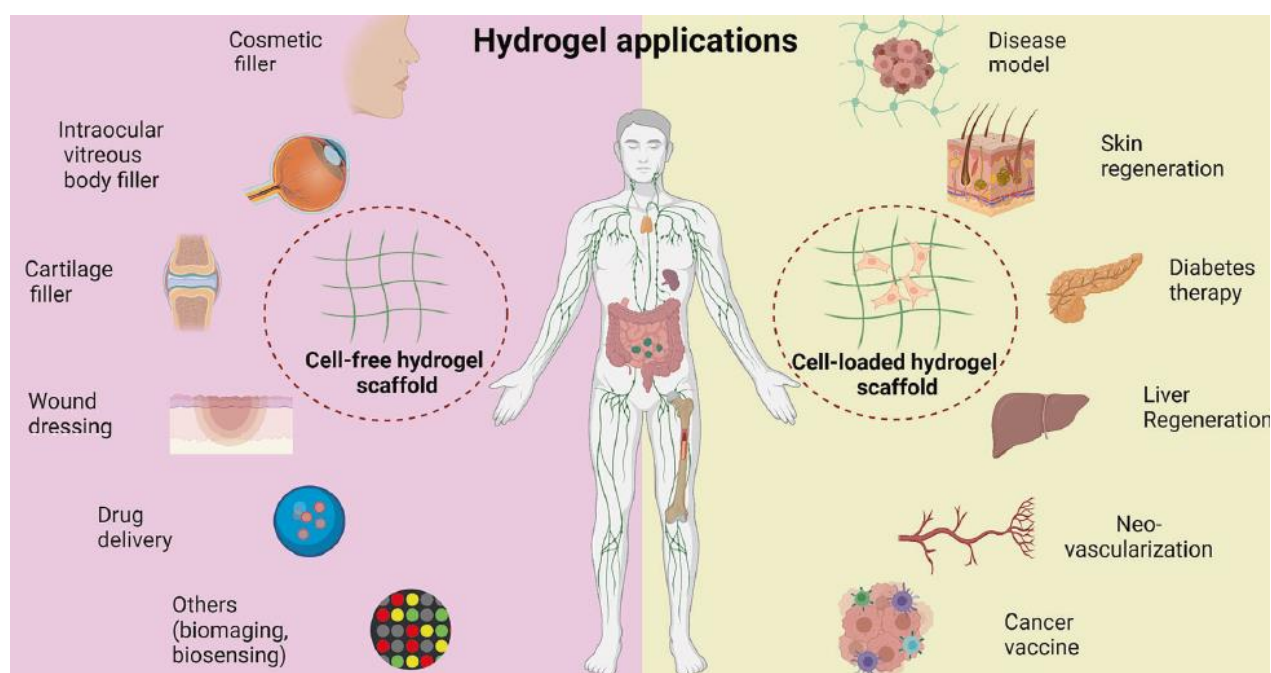
Figure 15: Diagram of biomedical applications for cell-free and cell-loaded hydrogels [32].

The polymeric network of hydrogels plays a crucial role in the interaction between cells and the surrounding environment, representing a key factor in the regulation of cell proliferation, migration, invasion, and other biological processes[30]. Hydrogels physical properties in fact, can modulate cell biology by altering the mechanotransduction signalling, which consists in the ability of cells to sense the external mechanical forces and convert them into biochemical signals that determine cells fate [32]. Several studies demonstrate that cells, thanks to the presence of specific mechanosensors as integrins and focal adhesion kinases, detect the hardness of the substrate and modify the contractility of the cytoskeleton depending on the cell-ECM adhesion forces [32]. It is

therefore important to regulate hydrogels rigidity according to the specific biomedical application through chemical cross-linking methods or nanoparticles doping, which are the two main strategies to improve mechanical properties [32]. Other parameters that influence cells behaviour are matrix pore size and the confinement established by the presence of the pores themselves, characteristics that affect especially the processes of cell division, differentiation and migration. It has been shown that cancer cells modify their migratory behaviour and adapt their metabolic activity depending on whether they experience confinement, as determined by the presence or absence of pores [32].
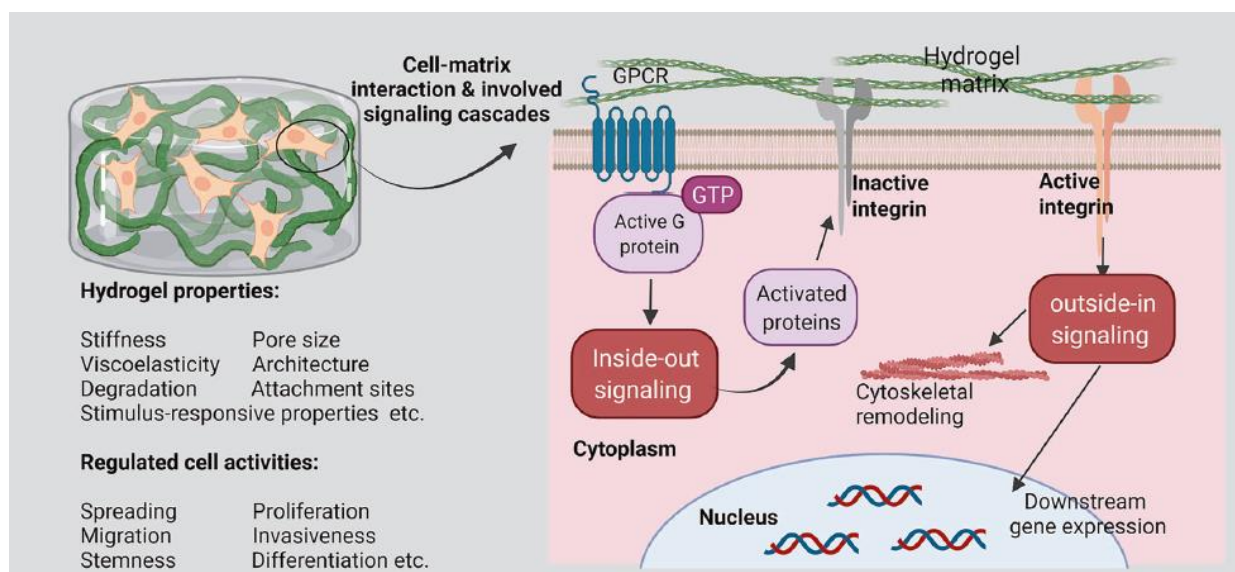
Figure 16: Schematic description of hydrogels' properties and effects on cell behaviours [32].

According to the source of polymers, hydrogels are grouped into natural, synthetic and semi-synthetic, inheriting different properties in terms of stiffness, stability, and biocompatibility [31]. Synthetic hydrogels ensure high reproducibility and mechanical strength but on the contrary of natural ones, are not biodegradable, bioactive and biocompatible [31]. Hydrogels can also be classified by the composition and configuration of the polymeric chains, the presence of ionic charges, the cross-linking method, and their response to external stimuli [31]. The classification based on the composition (homopolymer, copolymer, semi-interpenetrated and interpenetrated hydrogels) referees not only to the species of monomers that form the polymeric chains but also to the types of chains. Homopolymer hydrogels, composed by a single species of monomer, contain one type of polymer chain together with copolymer hydrogels, which derived from two or more species of monomers. Semi-interpenetrated and interpenetrated hydrogels are respectively characterised by one polymer network embedded in the liner polymer chains without cross-linking agents, and two or more polymeric networks linked by cross-linking agents [31]. The configuration of polymeric chains instead represents the organization of the network structures at

the molecular level, which is random for amorphous hydrogels, highly packed for crystalline hydrogels, and a combination of both in the case of semi-crystalline hydrogels [31].

According to the cross-linking methods, which are briefly summarized in Figure 18, hydrogels are classified into two more groups: chemical and physical. This process, which consists in polymer chemistry modifications, is necessary for the stabilization of the polymeric networks, enabling the formation and the subsequent degradation of the hydrogel structures [33]. Chemical hydrogels are characterised by permanent junctions between polymeric chains that makes them more stable under physiological conditions and more tuneable in degradation processes due to the presence of covalent bonds [33]. There are many chemical cross-linking methods of which the most common are: free-radical polymerization, high-energy reaction, and enzymes-induced cross-linking, all requiring a cross-linking agent[31]. The first two processes occur after the production of free radicals that are generally due to Ultraviolet (UV) and gamma ray excitation respectively, while enzymatic cross-linking depends on the enzyme concentration and it is widely employed in biomedical research for its rapid gelation under physiological conditions[31].Physical hydrogels instead, present transient junctions as hydrogen bonds, hydrophilic/hydrophobic interactions, polymerised entangles, and ionic/electrostatic interactions, through which softness and reversibility from liquid to solid are achieved [31], [34]. Despite their poor mechanical properties, these types of matrices are the most suitable for living cell encapsulation, therapeutic molecules delivery, ensuring high biocompatibility due to the absence of chemical reagents [34].
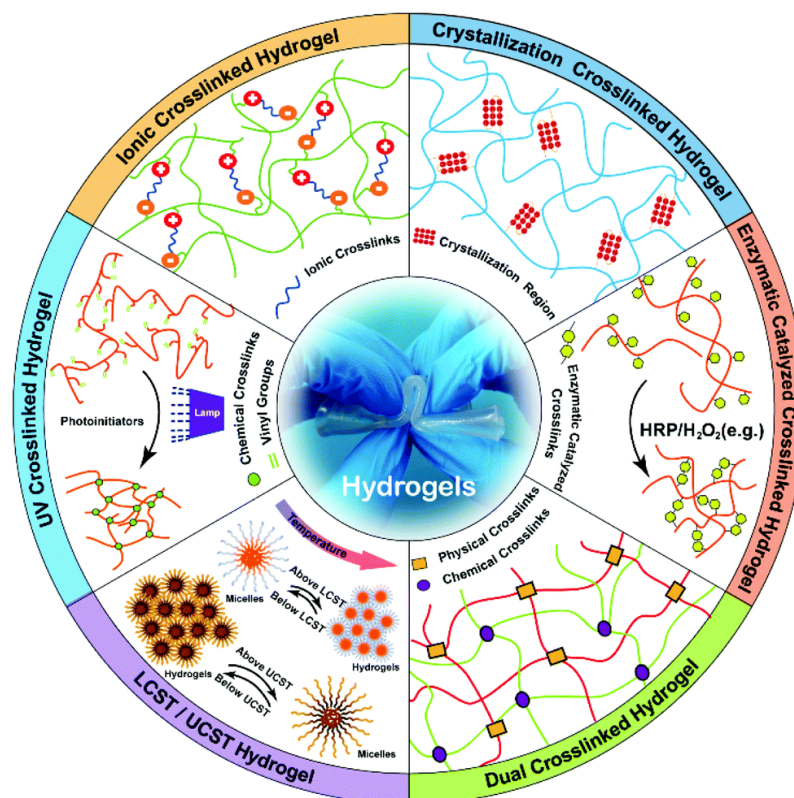
Figure 17: Principal crosslinking strategies for bioengineered hydrogels [34].

Finally, hydrogels are divided into two more categories depending on their ability to respond immediately to environmental stimuli: smart and non-smart hydrogels. These stimuli can be physical, as light, pressure, temperature, electric and magnetic field, chemical like pH variations and ion concentrations, but also biological/biochemical as in case of glucose-responsive hydrogels. The particularity of these matrices lies in their potential to act both as sensor and effector, by volume changes from the collapsed (unswollen) to the swollen state. For this reason, they are especially employed as drug delivery systems, able to protect drugs, peptides, and proteins from the external environment and to release these biomolecules in the correct time and concentration, overcoming the initial limitations of conventional drug delivery systems [35].
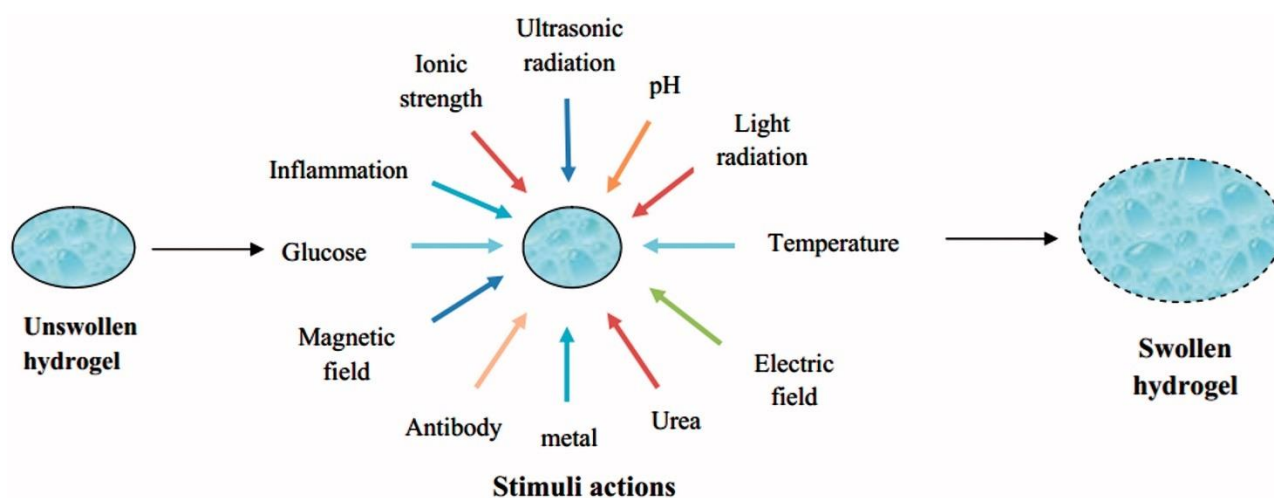
Figure 18: Mechanisms of action for smart swollen hydrogels [35].

One of the most versatile, not only for its tuneable biological and mechanical properties, but also from a processing point of view, is gelatine methacryloyl (GelMA)-based hydrogel. Due to the presence of cell-attaching and matrix metalloproteinase (MMP) responsive peptide motifs, this semi-synthetic hydrogel provides a biomimetic environment essential for cell proliferation and spreading[36].

1.3.4. GelMA-based Hydrogels and properties

Originally proposed by Van Den Bulcke et al.[37], GelMA is a biomaterial obtained from the chemical functionalization of primary amine and hydroxyl groups of gelatine chains with unsaturated methacryloyl groups to form transparent hydrogels through photo-polymerization [37]. Thanks to their excellent biocompatibility, biodegradability, and controllable photo-crosslinking properties, GelMA-based hydrogels have become a widely adopted platform both in drug delivery and tissue engineering applications.
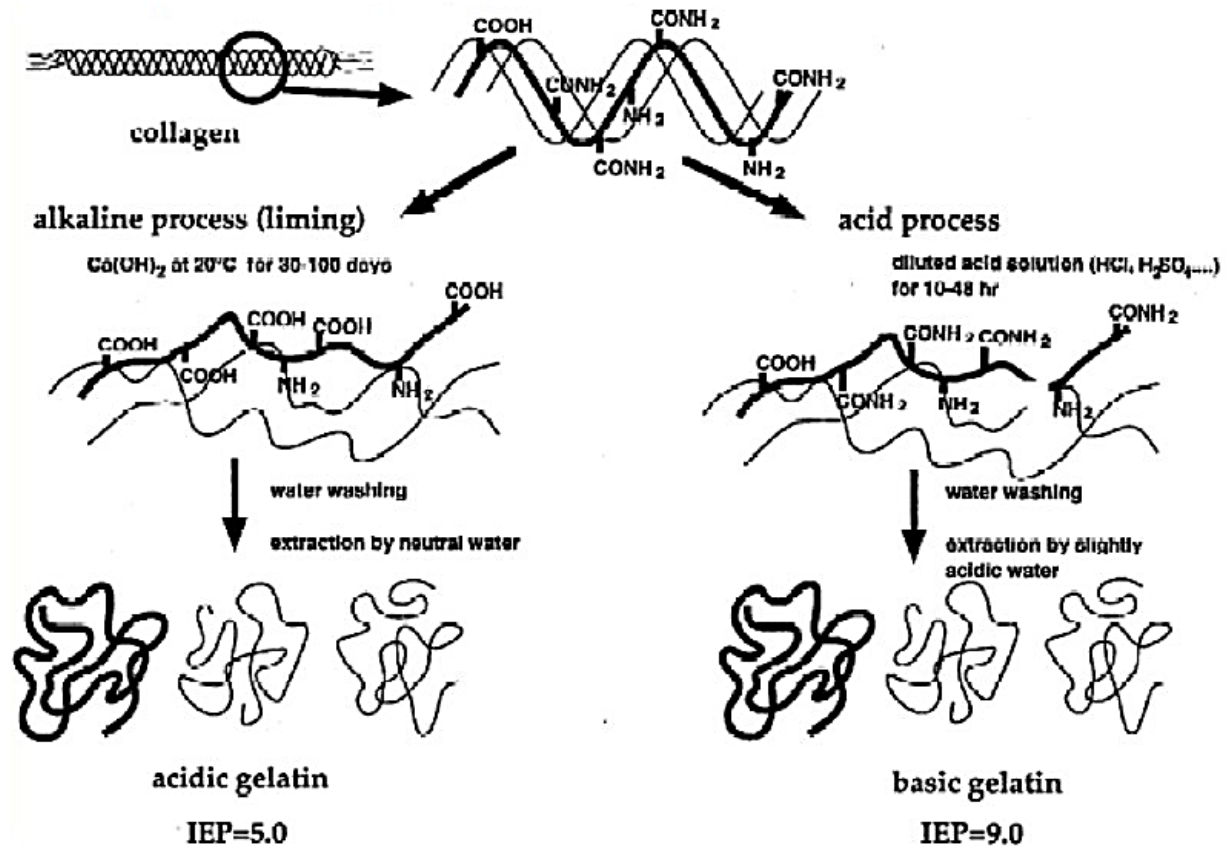
Figure 19: Diagram of production processes of Gelatine Type A (on the left) and Type B (on the right) and their typical isoelectric points (IEP: Isoelectric point).

GelMA is produced from gelatine, a thermo-responsive polymer obtained through the partial hydrolysis of collagen, responsible for the denaturation of its tertiary structure and the subsequent reduction of structural variations [36] . The extraction of gelatine, which is schematically reported in Figure 18, consists of several stages including pre-treatments based on acid, alkaline or sometimes enzymatic processes that influence the final type (A or B) of gelatine and therefore its properties [38]. Gelatine type A and type B exhibit different characteristics, not only as a result of their respective pre-treatment processes, acid for type A and alkaline for type B, but also due to their different sources which are porcine skin for type A and bovine one for type B. Moreover, while type A gelatine generally maintains collagen triple helix structure, type B is totally denatured and for this reason it has shorter gelatine chains [39]. Regardless of the type, gelatine not only

retains the repetitive amino-acid sequence of collagen (arginine-glycine-aspartic acid, known as RGD sequence) which is involved in cell-adhesion mechanisms, but it also acquires, in physiological conditions, a lower antigenicity and immunogenicity respect to collagen itself [38]. There are many advantages that make this natural-derived polymer one of the most investigated in biomedical applications such as its high availability at low costs, high biocompatibility, but also the in vivo reabsorption and the possibility of using it in different forms, from porous scaffolds to microspheres [38]. In addition, gelatine solutions can form physically cross-linked hydrogels due to their gelation property at low temperatures [36]. Nevertheless, pure gelatine that results in poor mechanical properties and highly solubility at body temperature, due to its low melting point of 31.7-34.2 °C [40], is often subjected to chemical modifications [38], [39].

The chemical process employed for GelMA synthesis is methacrylation, during which less than 5% of the amino-acid residues of gelatine react with methacrylic anhydride. Consequently, all the other functional amino-acid motifs, such as the RGD sequences, are not influence by the reaction, maintaining the intrinsic cell-adhesive properties of the original gelatine [36]. According to the amount of methacrylic anhydride added during the synthesis, the degree of functionalization (DoF) of GelMA results in three distinct categories: DoF of 60% (i.e., Low), of 85% (i.e., Medium) and of 100% (i.e., High), each of which shows different viscoelasticity properties [39]. Higher DoFs values in fact, leads to increased cross-linking density, resulting in tighter polymeric networks, characterized by decreased swelling rates [39], [41]. Some studies have investigated how methacrylic anhydride affects differently hydrogel DoFs, depending on the source of GelMA. In particular, GelMA synthetized from type A gelatine presents larger DoFs compared to GelMA derived from type B gelatine, probably due to the differing isoelectric point (IEP) of the two gelatines, which are pH between 7-9 and pH between 5-6 respectively [39]. The introduction of methacryloyl groups enables gelatine to undergo photo-crosslinking, leading to the formation of covalently cross-linked hydrogels [36]. The photo-polymerization process can take place at mild conditions (neutral pH, room temperature, aqueous environment, etc.) and consists in a free radical reaction that occurs in presence of a photo-initiator such as Lithium phenyl-2,4,6-trimethylbenzoylphosphinate (LAP), in an aqueous state [41]. UV irradiation of the photo-initiator brings to the formation of free radicals through homolytic cleavage that starts chain-growth polymerization. After this phase, chain propagation takes place among methacryloyl groups and terminates between a propagating chain and another free radical [41]. Compared to other methods, photo-polymerization results to be the most suitable approach for a spatiotemporal controlled generation of hydrogels [36].
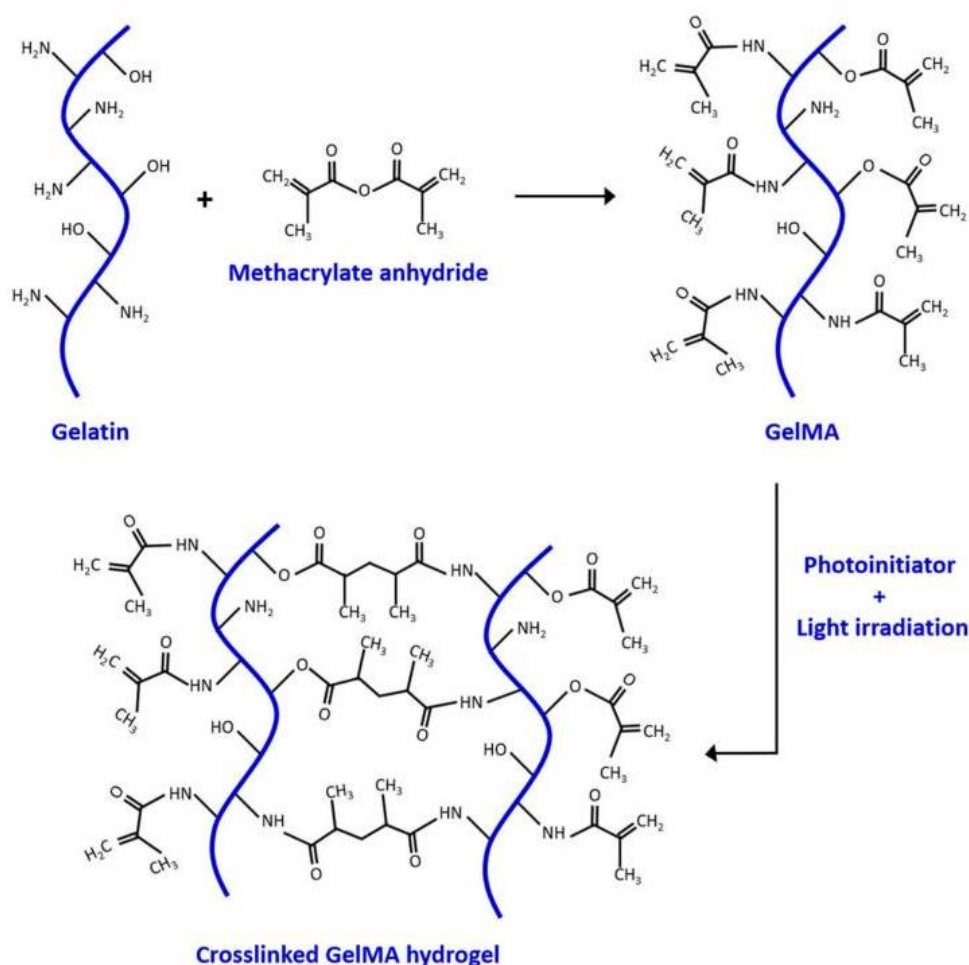
Figure 20: Illustration methacrylation of gelatine into GelMA and subsequent GelMA photo-polymerization into GelMA-based hydrogel [42].

To form cell-leaden 3D GelMA-based hydrogels, cells are suspended within the GelMA prepolymer solution before photo-polymerization occurs, which has been shown to preserve cell viability at 80%. For this reason, one of the main applications of this type of hydrogel is in vitro cell culture for modelling both physiological and pathological conditions. The possibility to provide more relevant environments, through the easy incorporation of TME's cells, to introduce microfluidic channels together with the affordable costs and the simple fabrication methods, make GelMA-based hydrogels powerful systems for cancer research[16] . However, in recent years, several microfabrication techniques based on these hydrogels, have been developed for the creation of tissue-like constructs that, through the inclusion of multiple cell types, closely resemble the complex architecture of native tissues [36]. In this context, cell response acquires high relevance and the opportunity to control it through the tuneability of the hydrogel mechanical properties, represent a significant advantage. Tissue-engineering represents therefore another biomedical field in which GelMA-based hydrogels can be employed, also due to their ability to retain their structural stability and physical form at body temperature [37].

Depending on the specific application, GelMA-based hydrogels can be formulated in different ways by varying synthesis parameters that significantly affect their mechanical and biological performances. Consequently, a comprehensive characterization is essential both to evaluate the material's suitability to the intended use and to clearly identify benefits and potential limitations. GelMA-based hydrogels can be characterized in terms of both physical and biological properties. The mechanophysical features, which include compressibility, hardness, stiffness but also porous degree and swelling behaviour, are exclusively governed by the set-up conditions which can be easily adjusted to achieve the desired requirements. In particular, the DoF, as well as the GelMA concentration and the photo-polymerization parameters, such as photo-initiator concentration, UV intensity and time exposure, can be all modulated to tune the hydrogel resulting properties.
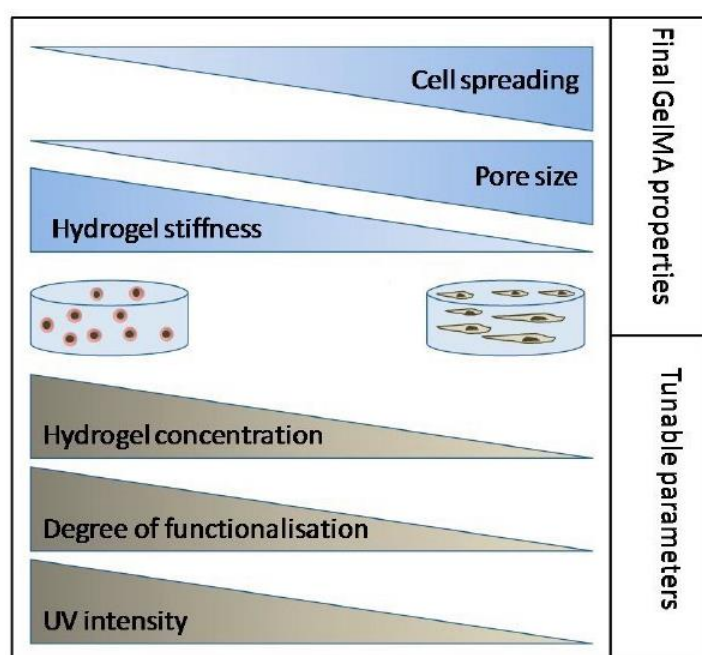
Figure 21: Graphical correlation between GelMA's biomechanical properties and its synthesis parameters [43].

Hydrogel stiffness, elastic modulus and adhesive strength, depend on GelMA concentration, which is directly proportional to the matrix softness. For example, GelMA samples prepared at 5% weight/volume (w/v) exhibit Young's modulus values that are approximately ten time lower than the same samples realized at 10% w/v. This difference is also reflected in the storage (G') and loss (G'') modulus, both of which increase with higher concentrations of GelMA [41]. While G' represent the quantity of energy needed to distort the sample, G'' correspond to the energy dissipated as the material returns in its original shape after the deformation. These parameters are employed in the rheological and photorheological characterizations, analyses through which viscoelasticity information are obtained by monitoring over time G' and G'' developments. For GelMA-based hydrogels, which are irreversible matrices, G' values are lower than those of G'' up

to the cross over point, at which sol-gel transition occurs. The transition depends on several factors, including not only the reaction temperature and the cross-linking agent concentration, but also what kind of material is analysed. The type of material in fact influences both the transition phase and the final value of G': GelMA derived from type A gelatine reaches higher values than the one from type B (31.6 ±2.0 kPa and 27.7 ±1.3 kPa respectively), highlighting the latter's lower rigidity and resistance [39]. On the contrary, the recovery rate, which is shown in Figure 22, consists in the capability of the hydrogel to restore the original viscosity after deformation, results to be better for GelMA originated from type B gelatine, whose viscoelastic values return to be 73%, 90% and 98% of the initial ones for High, Medium and Low DoF respectively [39]. GelMA type A instead is characterized by lower values, recovering in the first 20 seconds only 40% of the original viscosity [39]. Photorheological analysis, illustrated in Figure 22, reveals a clear dependence between G' and the DoF for both types of gelatine: higher DoFs corresponds to higher G' values [39]. This aspect highlights hydrogel's stiffness can be optimized by varying synthesis parameters.

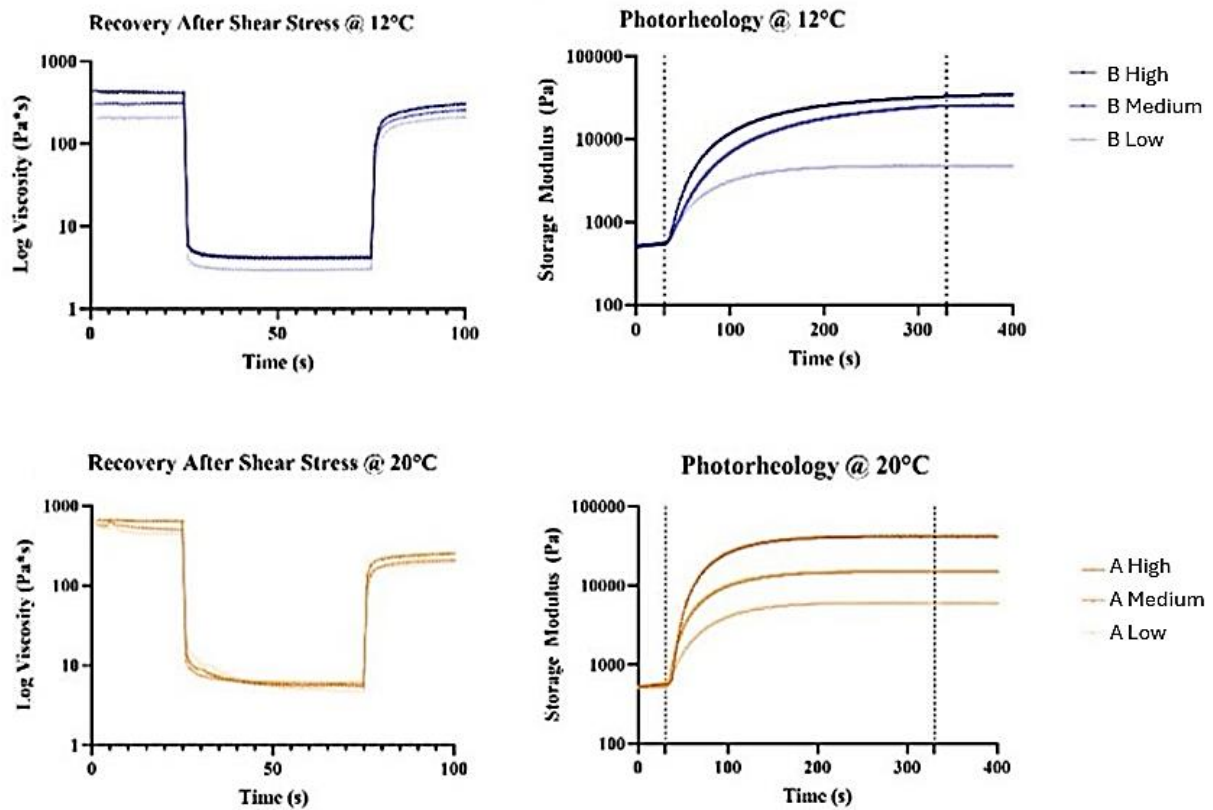Figure 22: GelMA type A (below) and B (above) photorheological and recovery rate characterizations [39].

GelMA concentration, together with DoF, plays a determinant role also in matrix porosity and thus in its pore dimension which generally varies between 50-100 μm (micropores) to 200-700 μm (macropores) [44]. The absence of vascular networks makes hydrogel pore size a critical factor for the proper diffusion of oxygen and nutrients, both essential to support cellular viability and therefore key processes as proliferation, migration and differentiation [44]. Moreover, if these hydrogels are employed as pathological in vitro models for drug testing, pore size has to be adequately controlled to provide an efficient diffusion of therapeutic agents. For GelMA-based hydrogels, this morphological feature can also be modulated through the regulation of UV intensity that is responsible for free radicals' generation. In particular, lower light intensity leads to a reduce free radicals' formation that slows the reaction kinetics, promoting homogeneous macrogel structures; higher intensity instead, brings to a greater and faster free radicals' production, allowing intramolecular cyclization and thus microgel patters creation, but negatively affecting cell survival [44].

In addition to UV intensity, other photo-polymerization parameters that can be externally controlled according to the specific cell subtype, are the concentration of cross-link agent and the exposure time. The first one is related to the hydrogel's cross-linking density: generally, higher photo-initiator concentrations lead to the formation of a greater number of propagating sites, resulting in shorter polymer chains and increased cross-links within the hydrogel network [41], [45]. The main consequences are the enhancement of material's rigidity and the reduction of its swelling capability, associated to limited water retention and lower oxygen and nutrient transport [39]. However, this behaviour is not always observed as in the case of LAP which provides hydrogels with improved mechanical properties at low concentrations [45]. Another aspect to consider when this cross-linking agent is employed, is the velocity of the polymerization kinetics, which results to be faster than those of other photo-initiators. This accelerated reaction may negatively influence the mechanical features of the matrix due to the generation of a heterogenous pore structure [45], [46].

In the same way as UV light intensity, also cross-linking concentration and duration result inversely proportional to cellular viability. Moreover, the exposure time shows a sigmoidal correlation with hydrogel tensile properties which increase as function of time, until reaching plateau trends at the end of cross-linking reaction. This indicates that, once the gelation process is complete, additional UV exposure does not further enhance the mechanical performance of the material [46].

In terms of biological characterization, enzymatic degradation assay represents a useful tool for the evaluation of material's stability against dissolution, whether by hydrolysis of the polymer or

through cleavage of the cross-linking [45]. This method consists of hydrogel incubation within collagenase XI solution that can interact with MMP-sensitive sites present in GelMA matrix [39] [45], [46]. The procedure involves an initial freeze-drying process to measure the undegraded sample weight, after which the sample itself is rehydrated for 24 hours to reach swelling equilibrium before being immersed in the collagenase solution. At the end of the assay, the GelMA sample is freeze-dried once again to obtain the degraded weight that is compared to the initial one, determining the percentage value of the residual mass [39]. Analysis results show that high resistance to enzymatic degradation is indicative of a greater cross-linking density. This evidence is supported by the fact that the process is slower the higher the GelMA concentration which, as previously discussed, is typically proportional to the degree of cross-linking network [46]. Moreover, also the UV time exposure influences the degradation kinetics that tends to be faster when the sample is irradiated for shorter periods of time [46].
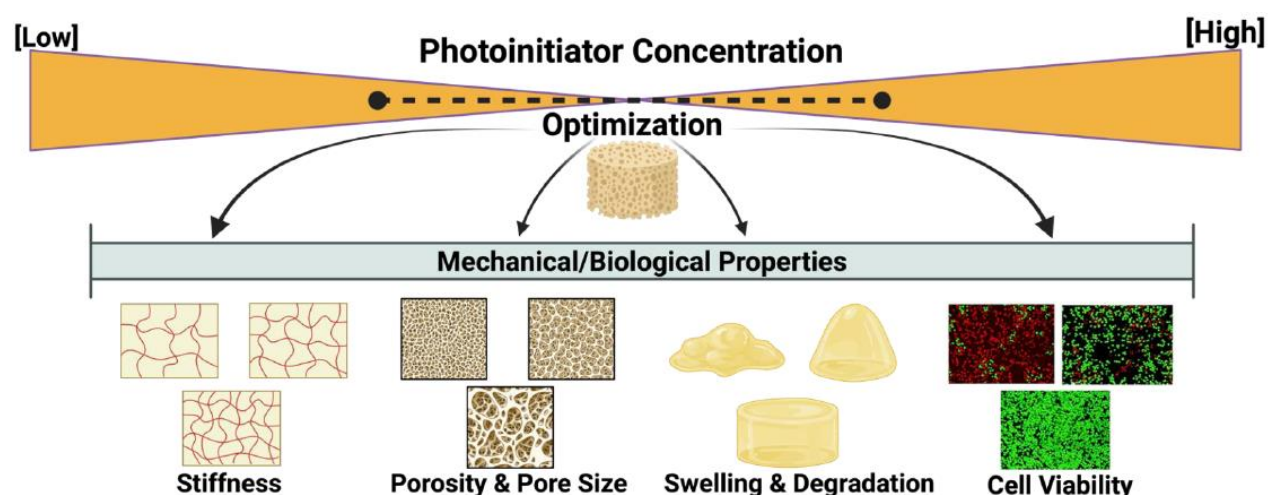

Figure 23: Influence of Photoinitiator concentration on the mechanical (stiffness, pore architecture, swelling behaviour) and biological (cell viability) properties of hydrogels [45], [46].

1.4. Aim of work

The aim of this thesis is to validate a GelMA-based hydrogel for 3D culture of mCRC patient-derived organoids, as an alternative to Matrigel the current gold standard in 3D modelling. An initial 3D in vitro study was performed using T84 mCRC commercial cell line, to determine whether type A or type B GelMA High DoF provided better support for adequate cell proliferation and viability. The best-performing GelMA type was selected for further investigations focused on analysing cellular behaviour within hydrogels characterized by the same polymer concentration but different DoFs. Specifically, T84 cells were cultured in type A GelMA High and Medium DoF hydrogels at 12,5% w/v concentration, to evaluate differences in cellular growth and morphology. After establishing the optimal GelMA DoF for 3D culture of commercial cell line T84, five mCRC patient-derived organoids were employed for the next steps based on comparing performances of type A GelMA Medium DoF hydrogels at 12,5%, 10%, and 7,5% w/v concentrations, in parallel with Matrigel. To identify which of the three GelMA formulations provided the most suitable microenvironment. Organoids proliferation and viability were assessed at 7 and 14 days of 3D culture while structural organization was evaluated at the same time points through digital and confocal analyses. Moreover, we investigated eventually different drugs response to Cetuximab and Trametinib, of patient-derived organoids when cultured in GelMA despite in Matrigel to highlight modifications in cell behaviour and to assess the effects of matrix composition on cell viability exposed to drugs.

Future perspective may include prolonged drug exposure studies to verify the consistency and reliability of therapeutic responses over time, but also the establishment of long-term 3D cultures to enable a more comprehensive evaluation of transcriptomic profiles fidelity of patient-derived organoids grown in GelMA-based hydrogels with the original tumour. These analyses could offer meaningful insights into the potential of GelMA-based hydrogels as physiologically relevant platforms for applications in personalized medicine and preclinical drug testing.

2. Materials and Methods

2.1. GelMA synthesis

GelMA synthesis is carried out following a specific and implemented protocol which can be used both to produce GelMA derived from type A (Bloom 300, Sigma Aldrich, G2500) and type B (Bloom 50-120, Sigma Aldrich, G6650) gelatine.

For the synthetization of GelMA type A, the first step consists in the realization of 100 ml of buffer solution, starting from 4 ml of carbonate solution (obtained by the dissolution of 1.1 gr of Sodium Carbonate in 50 ml distilled water (ddH2O)) and 46 ml of bicarbonate solution (originated by the dissolution of 0.84 gr of Sodium Bicarbonate in 50 ml of ddH2O), that are both added to 50 ml of ddH2O.

After this phase, through the use of a stirrer, that is set at 500 revolutions per minute (rpm) and at 50 °C, 10 gr of gelatine (Sigma-Aldrich) are dissolved in 100 ml of the buffer previously formed, and the pH of the solution is adjusted to 9.4 using sodium hydroxide (NaOH) at 5 molars (M) or chloridoid acid (HCl) at 5M.

When gelatine is completed melted, methacrylic anhydride (MAA, 94%) is added to the solution to obtain GelMA at different DoFs:

- 0.938 ml of MAA for DoF ≈ 100%;
- 0.705 ml of MAA for DoF ≈ 85%;
- 0.317 ml of MAA for DoF ≈ 60%.

At this point, the stirrer temperature is set at 55 °C and the solution is left for 1 hour, covered to prevent light influencing the process.

To stop the reaction, small amounts of NaOH 5M or HCl 5M are employed, in order to adjust the pH of the GelMA solution to 7.4.

The next step consists in a dialysis process with a total duration between 7 and 9 days. Dialysis membranes (Cellulose membrane, 12-14 kiloDalton molecular weight cutoff) are required.

The GelMA solution is pour into the membranes, leaving empty a little less than a half of each one, to avoid membranes' rupture during the process.

The membranes are left in ddH2O within the stirrer, whose temperature is set at 40 °C and its velocity rates at lower rpm. It is important to change ddH2O twice a day and make sure that the membranes are covered and do not leak during all dialysis.

The synthetization of GelMA type B follows the same steps, but using these amounts of MAA, the resulting DoFs will be slightly lower.

At the end of the process, solid porous structures characterized by disc shapes are obtained.

2.2. GelMA prepolymer solution

GelMA prepolymer solution, employed in photo-polymerization processes for GelMA-based hydrogels formation, is prepared in many steps through the use of:

- Complete Culture Medium
- Photo-initiator (LAP, Sigma-Aldrich)
- Synthetized solid GelMA
- Laboratory tubes (Centrifuge tube, Sorfa)
- Incubator
- Vortex mixer
- Magnetic stirrer
- Laboratory syringe 5 ml (InJ/Light)
- Laboratory syringe filters of 0,45 μm and 0,22 μm (Millex-HP, Millipore Express PES Membrane)

Complete Culture Medium is composed of 500 ml Dulbecco's Modified Eagle's Medium Nutrient Mixture F-12 HAM (DMEM/F12) to which are added:

- 10 mL of B-27 supplement (Gibco, 17504-044) 50X, final concentration 1X;
- 5 mL of N-2 supplement (Gibco, 17502-048) 100X, final concentration 1X;
- 1 mL of N-acetylcysteine (Sigma-Aldrich, A9165-5G) 500X, final concentration 1mM;
- 5 mL of Penicillin-Streptomycin (Sigma-Aldrich, P0781) 100X, final concentration 1X;
- 5 mL of L- glutamine (Sigma-Aldrich, G7513) 100X, final concentration 2 mM;
- 100 μL of EGF (Sigma-Aldrich, E9644) 100 ng/μL, final concentration 20 ng/m

Filtration using 500 ml Stericup, Quick Release-GP Sterile Vacuum Filtration System (Millipore S2GPU05RE) is required. Storage at 4 °C is needed.

First of all, the required amount of complete culture medium is collected into a proper lab tube and incubated at 37 °C to reach the appropriated temperature. Subsequently, LAP photo-initiator [2,5 mg/ml] is weight and added to the culture medium and mix through the use of a vortex mixer.

Meanwhile, solid GelMA is weighed and placed into a dedicated 50 ml laboratory tube in which, the solution previously prepared, will be added.

To ensure GelMA dissolution, the solution obtained is properly covered and left for 40 minutes in the magnetic stirrer, whose temperature is set at 60 °C.

The last steps involve two filtering to make the solution sterile carried out in biological safety cabinet: the first one through the use of laboratory syringe filter with 0,45 μm pore dimension and the second one by 0,22 μm pore dimension filter.

At this point, if GelMA prepolymer solution is not used immediately, incubation storage is required to prevent premature polymerization. Long-term storage instead is carried out in a refrigerator at 4°C with appropriate coverage.

To obtain 5 ml of GelMA prepolymer solution are needed 5 ml of Culture medium, 12,5 mg of LAP and:

- 625 mg for GelMA at 12,5% w/v concentration;
- 500 mg for GelMA 10% w/v concentration;
- 375 mg for GelMA 7,5% w/v concentration.

2.3. Tumour metastatic cell lines cultures

Tumour metastatic cell lines used in this study are LoVo and T84. The lines are grown in a humidified 5% CO_2 incubator at 37°C with two different culture mediums respectively:

- F-12K Medium (Kaighn's Modification of Ham's F-12 Medium) of ATCC that contains 2 mM L-glutamine and 1500 mg/L sodium bicarbonate, to which 10% w/v of fetal bovine serum;
- DMEM/F-12 of ATCC that contains 2.5 mM L-glutamine, 15 mM HEPES, 0.5mM sodium pyruvate, 1200 mg/mL sodium bicarbonate, to which 5% w/v of fetal bovine serum is added.

Cell lines were first cultured in 96-well plats within GelMA-based matrices, realized both with GelMA type A and GelMA type B. Two weeks cultures were performed to evaluate and compare their performance in supporting cellular behaviour.

The analyses consist in MTT assay to identify which hydrogel formulation provide a more suitable environment for cell growth, employing triplicates for each condition and control samples. Data are recorded at day 1, day 7, and day 14 after cellular seeding. Live/Dead staining is performed to qualitatively quantify organoids viability, while confocal microscopy to evaluate the influence of each composition on the morphological features of the cultured cells.

2.4. Development of Metastatic Colorectal Cancer Patient-derived organoids and 3D Matrigel culture

In this study, mCRC organoids derived from XENTURION platform, are employed to identify which GelMA formulation is the most suitable as a valid alternative to conventional matrices used for organoids culture. XENTURION, which is a living biobank of 128 patient-derived xenografts (PDXs) and paired tumoroids from mCRC samples, represents a significant resource for large-scale and well-powered preclinical cancer studies. The majority of these models were subjected to multiple comparative analysis at the mutational, genomic and transcriptomic levels, demonstrating high degree of intra-pair similarity. Moreover, XENTURION models preserve the genetic heterogeneity of the original tumour, exhibiting resistance to the same therapy (anti-EGFR antibody cetuximab ex vivo and in vivo) and displaying the same somatic variants and CNAs observed in clinical datasets of mCRC. Stepwise drug screening is also required to evaluate the efficacy of specific compounds against candidate target, first in patient-derived tumoroids and in PDXs for the final validation [47].

Figure 24: Schematic overview of XENTURION experimental design[47].

Organoids were generated both through tumour specimens collected from donor patients treated by liver metastasectomy and PDX explants. In each case, the protocol followed is the same and consists in a beginning step in which sample are minced and then washed with Phosphate buffered saline (PBS). Subsequently, centrifugation is required to obtain cell preparations that are embedded for 10-20 minutes at 37 °C in Corning Matrigel Growth Factor Reduce (GRF) Basement Membrane Matrix (LDEV-free, 10 ml, Product Number 354230) or Culture Basement Membrane Extract (BME Type II or Ultramatrix RGF BME, R&D System) before complete organoid medium

is added. Organoids are cultivated in 6-well plates and maintained at 37 °C in a humidified atmosphere of 5% CO_2 [47].
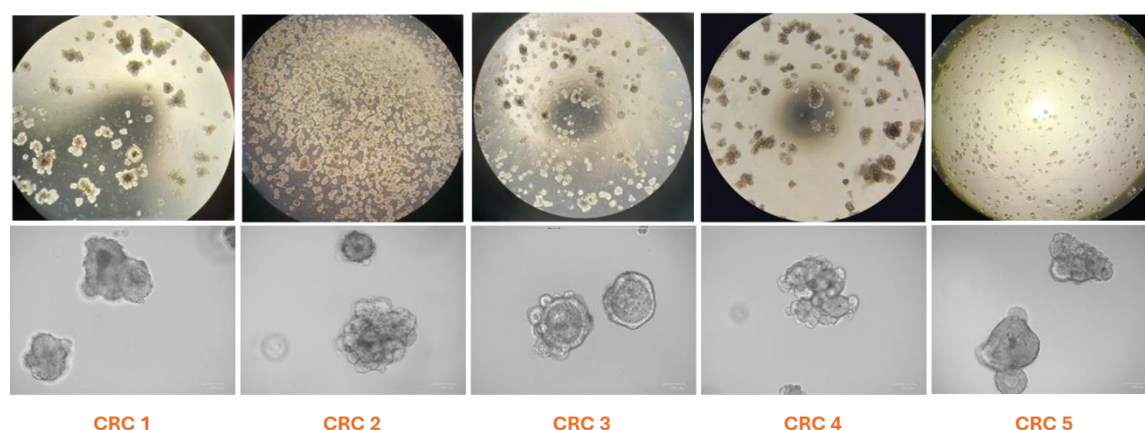

Figure 25: Microscopy imagines of the five mCRC patient-derived organoids employed.

The experimental protocol employed in this study includes an initial dissolution and removal of Matrigel domes, in which organoids are embedded, as well as their subsequent dissociation. The process involves the use of:

- PBS (Dulbecco's Phosphate Buffered Saline, 500 ml (Sigma-Aldrich, D8537) 1X
- Complete Culture medium
- Tissue culture treated multi-well plates (Costar, 6 well cell culture cluster)
- Laboratory tubes (Falcon 15 mL High-Clarity Polypropylene Conical Tube, 352096)
- Trypsin 2,5X
- Trypan Blue staining (1:8)
- Vacuum pump
- Incubator
- Centrifuge

The first step consists in the Matrigel dissociation, using a laboratory pipette, through culture medium and small amount of PBS. Samples are then collected in specific 15 ml laboratory tubes and by adding PBS are brought to the same volume.

Centrifugation at 4 °C and 1300 rpm for 5 minutes is required.

Subsequently, the supernatant is removed thanks to a vacuum pump and, for each sample, 1 ml of trypsin is added to the pellet obtained before.

Incubation at 37 °C for 5 minute is needed.

At this point, to block trypsin's action 1 ml of culture medium is added.

Cell counting is carried out through trypan blue staining.

From each sample, a specific volume is then taken based on cell counting to have a final cells concentration of 3000 cells/well.

PBS is added to adjust all samples to have the same volume.

Second centrifugation at room temperature and 1300 rpm for 5 minutes is performed.

Supernatant is subsequently removed through vacuum pump, and samples are resuspended by adding complete culture medium in the desired final volume which is 50 μl for seeding 40 wells.

To this solution are added 1950 μl of Matrigel, which must be kept on ice during all the process.

At this point, 50 μl of the solution are seeded in 96-well plates.

Polymerization occurs in incubator at 37 °C for 15-30 minutes approximately.

After that, 200 μl of culture medium are added to each sample.

Long-term culture at 37°C is performed.

Matrigel culture plans to consider five patient-derived mCRC organoids.

2.5. Patient-derived mCRC organoids 3D culture in GelMA-based hydrogels

Culture in GelMA-based hydrogels of patient-derived mCRC organoids follows the same steps describe in previous paragraph (2.4.), except that, after the second centrifugation and resuspension in complete culture medium, specific volumes of GelMA are added to the solutions.

At this point, 50 μl of the solution are planted in 96-well plates and polymerization is carried out through the use of UV crosslinker at 365 nm for 45 seconds.

After polymerization, 200 μl of complete culture medium are added to each sample.

Long-term culture at 37°C is performed.

GelMA-based hydrogels culture plans to consider five patient-derived mCRC organoids.

2.6. Morphological characterization

Morphological characterization refers to qualitative and quantitative analyses that in this thesis are focalised on the description and evaluation of features as shape, dimension, structure and organization of patient-derived mCRC organoids cultured within both GelMA-based matrix and Matrigel. The investigation of these aspects plays a pivotal role in the determination of GelMA-based hydrogel's effectiveness as an adequate 3D model for the promotion of cell-cell interactions, essential biological functions and tissue-like organization.

Analyses are carried out through two distinct devices:

- Digital imaging system (ZOE Fluorescent Cell Imager, BIORAD);
- Confocal spinning disk microscope (Crest X-Light).

The first one, employed in Brightfield channel modality, is useful not only to observe organoids' shape but also to evaluate the structural integrity and distribution, enabling at the same time, the estimation of their size. For a more detailed analysis of the internal structure instead, confocal spinning disk microscopy is adopted. This instrument allows advanced optical imaging through which the development of 3D images, the quantification of fluorescence signals and the simultaneous visualization of multiple markers are possible. In this case, confocal microscopy is used to detect and distinguish subcellular structures of organoids thanks to the use of three different fluorescent stains:

- DAPI (4′,6-diamidino-2-phenylindole), for nuclei visualization;
- Phalloidin, for cytoplasm and cells' morphology visualization ;
- Wheat Germ Agglutinin (WGA), for plasmatic membranes visualization.

Staining protocols typically include a prior fixation step. The standard procedures are illustrated in the next paragraphs.

Confocal microscopy employs duplicates for each sample. The analysis involves the extraction of samples from each well using laboratory scoop and the subsequent location onto Petri dish supplemented with small amounts of PBS to keep them hydrated during the confocal analysis. The imagines were acquired using 20X objective lenses to discriminate all the organoids' components.

2.6.1. Fixation protocol

Fixation preserves cells in their current state by stabilizing their structure and morphology, and it is essential to make them permeable, allowing effective penetration of the staining agents.

The fixation protocol requires:

- PBS 1X
- Paraformaldehyde 4% (Thermo Scientific) (PAF)
- Laboratory rocker

The first step consists in culture medium removal, followed by two 5-minutes washes in PBS on the laboratory rocker, to ensure complete elimination of any residual medium.

The samples are then incubated with PAF (200 μl for each sample), pre-warmed at room temperature, for approximately 30-40 minutes.

After fixation, the PAF removal is performed and two additional washes under the same condition are needed.

Long-term storage before staining is carried out in PBS at 4°C.

2.6.2. Staining protocol

The staining protocol requires:

- PBS 1X
- DAPI (Sigma-Aldrich) 1μM
- Phalloidin (Sigma-Aldrich) 0.25 μM
- WGA (Sigma-Aldrich)
- Triton X-100 (Sigma-Aldrich) 0.25% volume/volume (v/v)
- Laboratory rocket

Starting from the previously fixed samples and after PBS removal, 200 μl of WGA is added to each well, and then samples are incubated in the dark on the rocking platform for 1.5 hours at room temperature.

A subsequent 5-minutes wash with PBS is performed on the laboratory rocket at room temperature, followed by the addition for each sample of 200 μl of Triton X-100. Dark incubation on the rocking platform for 30 minutes is required to ensure selective membranes' rupture which contribute to cellular permeabilization.

At this point, two 5-minutes washes with PBS are needed before the next incubation with 200 μl for each well of DAPI-Phalloidin solution in PBS (DAPI 1:500, Phalloidin 1:1000), which is performed under the same conditions for 4 hours.

Finally, one 5-minutes wash with PBS is required.

2.7. Proliferation assay

Proliferation assay represents an essential tool to quantify and monitor cellular development in many biomedical applications such as *in-vitro* research, preclinical drug testing, cytotoxicity studies and regenerative medicine. In this thesis, MTT assay is employed to detect the proliferation of T84 cell line and mCRC patient-derived organoids, providing quantitative results as optical absorbance values. In particular, MTT assay, which is briefly illustrated in Figure 26, is employed to quantify metabolically active cells after the incubation with a mono-tetrazolium salt, able to penetrate both through the cell membrane and the mitochondrial inner membrane, due to its positive charges and lipophilic properties. Inside living cells, the salt is reduced into formazan, resulting in the formation of a violet-blue, water-insoluble compound which is then solubilized by a specific solvent. The optical absorbance of MTT-formazan solution is read at specific wavelengths, through the use of a micro-plate reader. This measure provides an indication of formazan concentration, which reflects the intracellular MTT reduction and, consequently, cell viability [48].
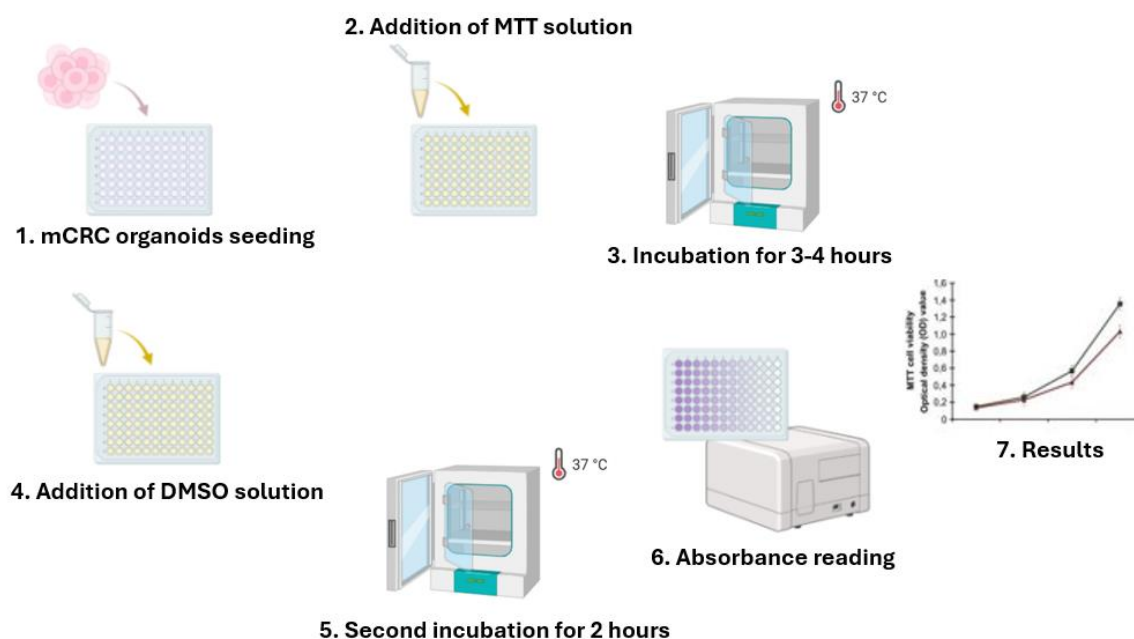

Figure 26: Workflow of MTT assay procedure

The MTT assay performed on T84 cells grown in GelMA-based hydrogels, employs triplicates of each condition, while for mCRC patient-derived organoids cultured both in GelMA-based hydrogels and in Matrigel, five replicates for each organoid and five control samples are used. The experimental design is illustrated in Figure 27. The MTT analysis is conducted at 1 and 7 days of cellular seeding for T84 cells, and after 7 and 14 days of 3D culture for organoids.
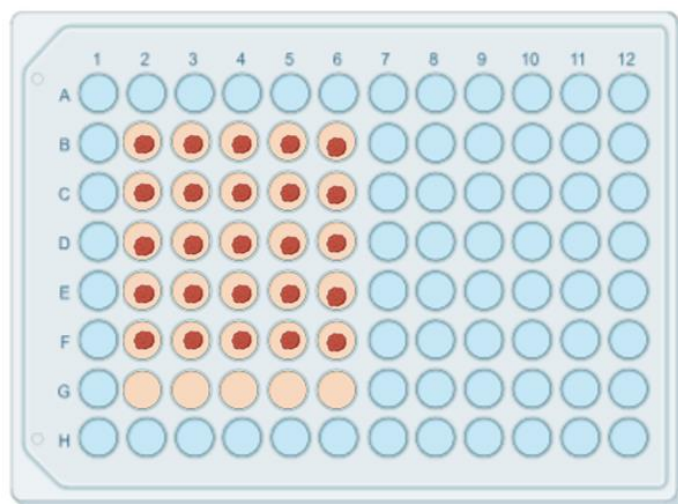

Figure 27: Experimental set up for five patient-derived mCRC organoids culture.

The protocol employed in this study for 3D cell culture includes:
- Complete Culture Medium
- MTT reagent (Sigma-Aldrich) 0.5mg/ml
- Dimethyl sulfoxide (DMSO) (Sigma-Aldrich)
- Micro-Plate reader (Biotek)

The first step consists in the removal of culture medium from each sample, and the subsequent addition of 200 μl for each well of a solution composed by MTT and complete culture medium (1:10). Dark incubation at 37°C for 3-4 hours is required.

At this point, after the solution removal, the addition of 200 μl for each well of DMSO is performed. Dark incubation at 37°C for 2 hours is carried out.

The final phase includes the measurement through the micro-plate reader of the samples' absorbance at two different wavelengths:
- 570 nm, wavelength at which the MTT-derived formazan solution absorbs the most
- 650 nm, reference wavelength used to correct background.

The final absorbance of each sample is obtained by subtracting the reference wavelength values from those measured at 570 nm.

2.8. Viability assays

Viability assays constitute commonly approaches used to evaluate the proportion of living cells within a culture and determine if biomaterials or experimental conditions can affect cell survival. In this thesis are employed: Live/Dead assay, a qualitative fluorescent-based method which allows a clear discrimination between live and dead cells, and Cell Titer Glo Luminescent 3D assay that is used for determining the number of viable cells by quantifying levels of intracellular adenosine triphosphate (ATP), a reliable marker of metabolically active cells. The Live/Dead assay is based on two fluorescent dyes: Calcein-AM, which stains live cells green via esterase activity (λex 490 nm, λem 515 nm), and Propidium iodide, which labels dead cells red by binding to DNA in cells with compromised membranes (λex 535 nm, λem 617 nm). Both dyes can be excited at 490 nm, allowing simultaneous visualization of live and dead cells under a fluorescence microscope. The Cell Titer Glow Luminescent 3D assay instead, employs a single reagent able to lyse cells which release ATP triggering a luciferase-catalysed reaction that produces a luminescent signal proportional to the number of viable cells.

2.8.1. Live/Dead assay

The Live/Dead assay is performed on T84 cell line cultured within GelMA-based hydrogels after 7 days of cellular seeding, and on mCRC patient-derived organoids grown both in GelMA and Matrigel, at 7 and 14 days of 3D culture. For both analyses, duplicates of samples are considered. The protocol used includes:

- PBS 1X
- Calcein-AM solution (solution A, Live/Dead Cell Double Staining Kit, Merck)
- Propidium iodide solution (solution B, Live/Dead Cell Double Staining Kit, Merck)
- Laboratory rocket
- Incubator
- Laboratory scoop
- Petri dish
- Confocal spinning disk microscope

After the removal of culture medium from each sample, two consecutive 5-minutes washes for each sample on the laboratory rocket at room temperature are needed to guarantee complete elimination of any residual medium.

The next step consists in the addition of 200 µl for each well of a solution composed by PBS, solution A (1:500) and solution B (1:1000). Dark incubation at 37 °C for 30 minutes is required.

Before confocal microscopy, another 5-minutes wash in the dark is performed and then 200 µl of PBS are added to each sample.

Samples are subsequently collected from each well using laboratory scoop and transferred onto Petri dish supplemented with small amounts of PBS to keep them hydrated during the confocal analysis. The imagines were acquired using 20X objective lenses in order to capture an overview of live organoids.

2.8.2. Cell Titer Glow Luminescent assay

The Cell Titer Glo Luminescent assay is performed on mCRC patient-derived organoids cultured both in GelMA and Matrigel. It is used on untreated and treated samples after 72h from drugs administration. The protocol includes:

- Cell Titer Glo reagent (Promega)
- Laboratory rocket
- Incubator
- White 96-well plates (Nunc Maxisorp, Merck)
- Micro-Plate reader (Biotek)

After the removal of culture medium from each sample, 100 µl of the reagent are added. Dark incubation at room temperature for 20 minutes on the laboratory rocket is required.

Subsequently, 200 µl of solution from each sample are collected and transferred to the white 96-well plates for luminescent acquisition.

2.9. Drugs response

The evaluation of drug administration in organoids 3D models is becoming a crucial aspect to assess whether hydrogel composition and its biomechanical properties in presence of drugs can induce changes in organoids proliferation levels, morphological features, or mutational profiles. The last part of the thesis is focused on studying the effects of two distinct drugs on organoids culture: *Cetuximab* and *Trametinib* (Selleckhem). The first one is employed in EGFR target therapy, resulting ineffective in case of KRAS and NRAS mutations, which are found in all the five mCRC patient-derived organoids employed in the study. The second one is applied for BRAF targeted therapies due to its ability to inhibit MEK pathways. The efficacy of this treatment in mCRC patients with the mutations previously cited is currently under investigation.

Drug treatment is performed on organoids cultured in type A GelMA Medium DoF hydrogel at 7,5% w/v concentration and in Matrigel. After 7 days of 3D culture, the medium is replaced with 200 μl of fresh complete culture medium supplemented by the specific drug to obtained a final concentration of 20μg/ml and 50nM for Cetuximab and Trametinib, respectively. For control samples, the replacement of the medium is performed at the same time point.

CTG Luminescent assays and digital microscopy are used to investigate organoids viability and morphology changes at 72 h from treatments.

3. Result and Discussion

3.1. Tumour metastatic commercial cell lines 3D culture in GelMA-based hydrogels

For setting up the experimental platform we employed T84 mCRC commercial cell line, derived from lung metastasis, and investigated two different kinds of GelMA, type A and B, both with High DoFs and 12,5% w/v concentrations. Two weeks of 3D cultures were performed to evaluate cell behaviours within type A and B GelMA-based hydrogels and then validate the one which best supports spheroids formation and growth.

Proliferation rate was evaluated after 1 and 7 days of 3D culture, showing how T84 cells since the first 24h up to 7 days of culture, exhibited higher proliferation in type A GelMA compared to samples cultured in type B one. Specifically, T84 cells in type A GelMA increased by approximately 40% from day 1 to day 7, while growth in type B GelMA resulted extremely low with an increment by only 5%. Specifically, the proliferation from day 1 to day 7 expressed in fold increase resulted of 1.04 for type B GelMA and of 1.4 for type A GelMA, reflecting enhanced proliferation between the two time points (Figure 28).
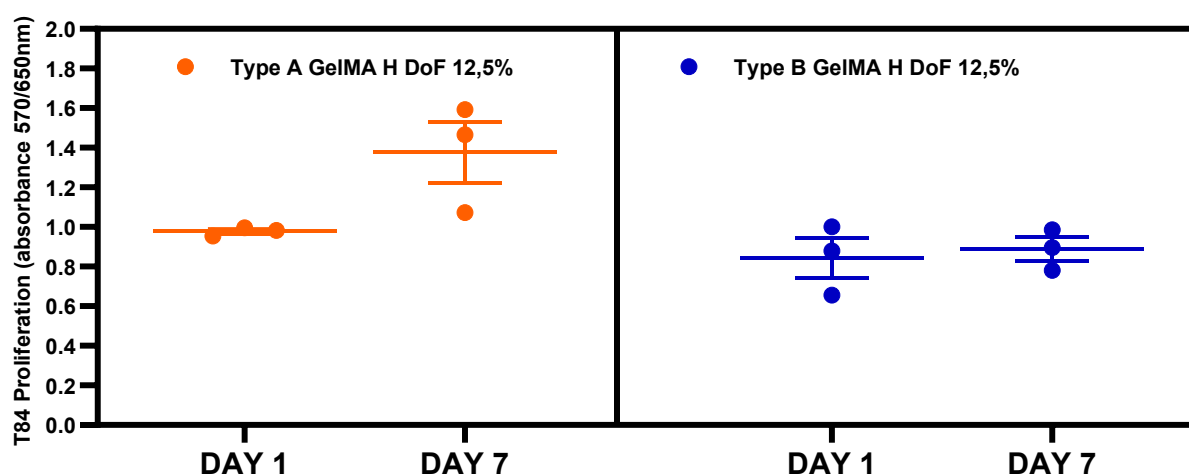

Figure 28: T84 cells proliferation in Type A and B GelMA-based hydrogels High DoF at 12,5% w/v concentration, at day 1 and 7 of 3D culture. Absorbance values are normalized against the blank at the two time points (n=3).

To further evaluate cellular viability, a Live/Dead assay of T84 cells cultivated within type A and B GelMA-based hydrogels, was carried out on day 7. The confocal analysis revealed a complete absence of cell mortality in samples grown in type A GelMA, whereas the counterpart grown in type B highlighted a reduction in cell survival as evidenced in the representative pictures of Figure [], by the presence of numerous dead cells (red). Additionally, the population of viable cells (green) in type B hydrogel is significantly lower compared to the previous condition (Figure 29).
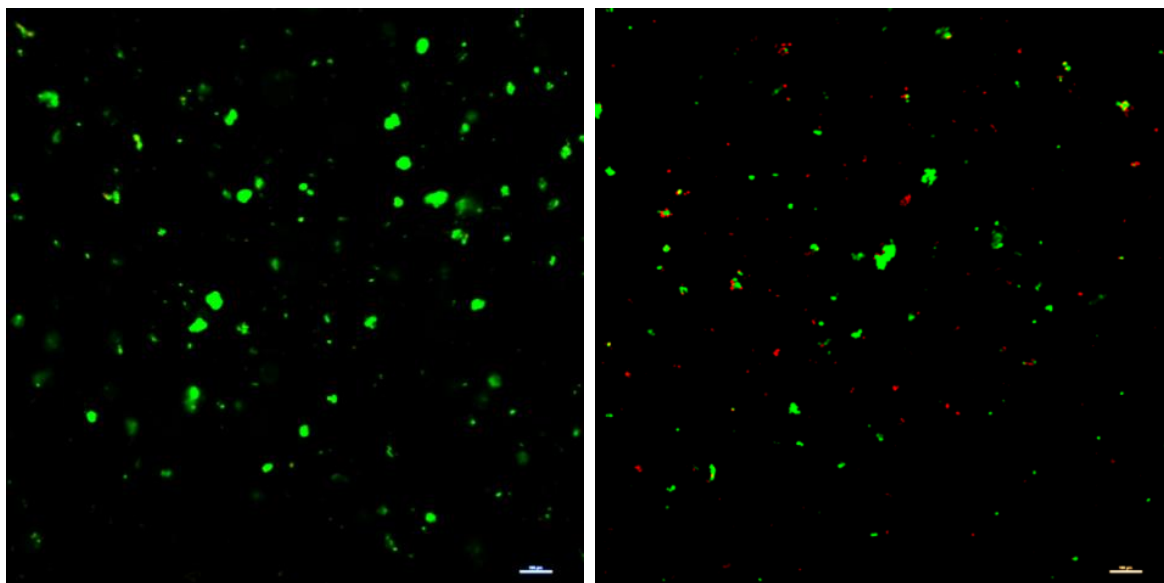
Figure 29: Representative picture of Live/Dead staining (4X objective lens) showing the viability (green) and death (red) of T84 cells cultured in type A (on the left) and type B (on the right) GelMA-based hydrogels High DoF at 12,5% w/v concentration, at day 7 of 3D culture. (Scale bar: 500 µm).

These preliminary analyses indicate that, despite identical DoF and GelMA concentration for both conditions, type A provides a more favourable microenvironment for the development of T84 cells. A possible explanation could lie in the different chemical characteristics of the materials at physiological pH (7.4), which corresponds to the pH of the culture medium. When the pH of the solution in which hydrogels are embedded is lower than the IEP of the polymer, its functional groups become protonated, resulting in a net positive surface charge, and vice-versa [49]. Type A GelMA presents IEP around 9 (as type A gelatine), therefore carries a positive charge that promote cells-matrix interactions, due to the negative charge of cell membrane.

Next step was to assess how modification in the DoF of GelMA could influence the T84 cells proliferation capability and their morphological features. Therefore, we investigated two formulations of type A GelMA both with 12,5% w/v concentration but characterized by different DoFs: High and Medium which principally differ in the amount of methacrylic anhydride added during GelMA synthesis, higher and lower respectively. For both matrices, proliferation rate was recorded at 1, 7 and 14 days of 3D culture. While between day 1 and 7 the proliferation was maintained similar in both matrices, between 7 and 14 days of 3D culture, T84 cells showed to better growth in type A GelMA Medium DoF than in the High one, with an increase in proliferation of the 52% and 24%, respectively. Lower proliferation capability in GelMA High DoF could probably be due to its higher cross-linking density and consequently reduced hydrogel's pore size. These characteristics compromise processes as cell-cell interactions and migration, negatively affecting cellular growth [50].

Morphological analyses were performed by confocal spinning disk microscope after DAPI-Phalloidin-WGA staining of T84 cells in type A GelMA High and Medium DoF at 12,5% w/v concentration at day 14 of 3D culture. T84 cells grown in GelMA hydrogels at 10% w/v concentration showed greater tendency to agglomerate, forming well-defined masses, morphologically similar to 3D spheroids and organoids, while cells cultured in the other GelMA formulation displayed poorer structural organization and reduced size (Figure 30).
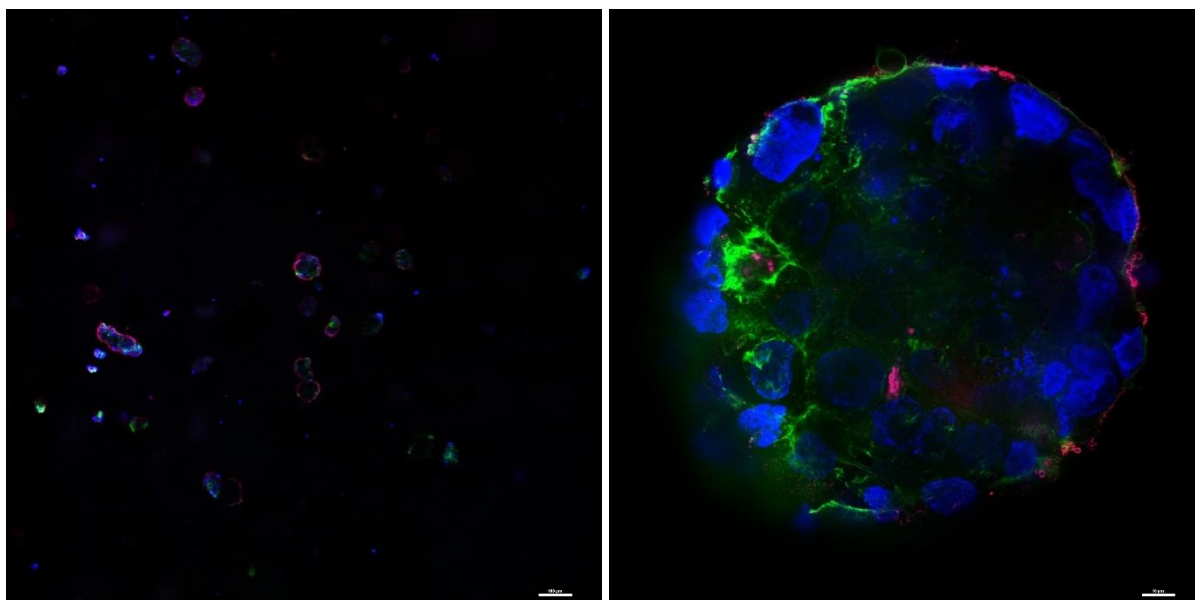

Figure 30: Representative picture of DAPI-Phalloidin-WGA staining (20X objective lens) showing nuclei (blue), cytoskeleton (green), and plasmatic membrane (pink) of T84 cell line cultured in type A GelMA High (on the left) and Medium (on the right) DoF at 12,5% w/v concentration, at day 14 of 3D culture. (Scale bar: 100 μm).

Hydrogels based on type A GelMA Medium DoF at 12,5% w/v concentration offered a more adequate microenvironment for the culture of T84 cell line, performing improved biological compatibility and enabling higher cellular growth.

At this stage, we conducted our next experiments by substituting mCRC commercial cell line with primary tumour cells, moving toward the identification of the optimal GelMA conditions in terms of DoF and w/v concentration for patient-derived organoids.

3.2. Patient-derived mCRC organoids 3D culture in type A GelMA-based hydrogels

To investigate the potential of type A GelMA-based hydrogels, primary biological material was employed. Five patient-derived mCRC organoids (CRC1, 2, 3, 4, 5), all KRAS/NRAS mutated, were cultivated over 14 days in type A GelMA Medium DoF with three distinct polymer concentrations, 12,5%, 10%, and 7,5% w/v and also in parallel with Matrigel, with the aim of determine which of the three formulations best support organoids organization compared to the current gold standard matrix. Morphological analysis is in fact a key approach for organoids characterization, offering detailed insights into their structures and features with systems such as digital imaging and spinning confocal disk microscopy. Proliferation and viability assays were performed to obtain supporting data.

3.2.1. Type A GelMA Medium DoF at 12,5% versus 10% w/v concentration

3D cultures of the five mCRC patient-derived organoids were performed within type A GelMA Medium DoF hydrogels at 12,5% and 10% w/v concentrations, and proliferation rate was evaluated after 7 and 14 days of 3D culture. Figure 31 shows for each patient organoid the proliferative trends expressed as *fold increase* between 7 and 14 days after 3D culture.
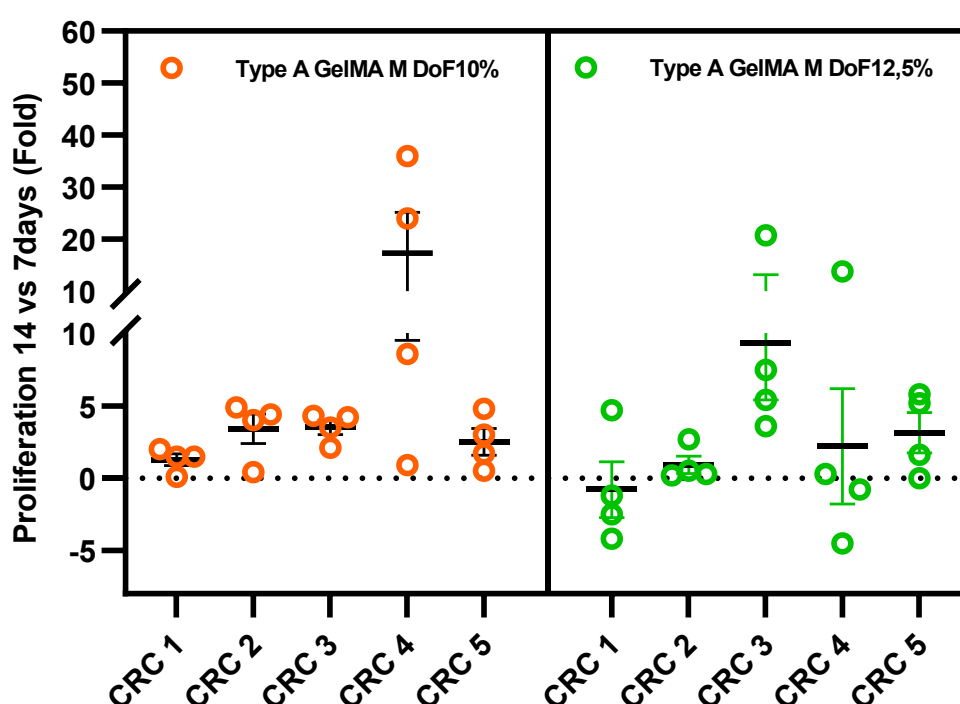

Figure 31: Proliferation expressed in fold Increase between day 14 and day 7 of mCRC patient-derived organoids grown in type A GelMA Medium DoF hydrogels at 12,5% and 10% w/v concentrations (n=4).

All samples grown in GelMA-based hydrogel at 10% w/v concentration, exhibited a good proliferation rate always major than 1, indicating an overall implementation in cellular

proliferation over time. Moreover, 3 out 5 patients, CRC 1, 2, 4, showed a better capability to grow when cultured in GelMA at 10% w/v concentration; in particular CRC 4 was characterized by values up to 8 times greater than in the other formulation.

On the contrary, CRC 2 and CRC 1 grown in GelMA at 12,5% w/v concentration showed on average a proliferation fold increase lower than 1, 0.9 and -0.8, respectively, underlying a reduction in cell survival. Moreover, samples cultivated within GelMA at 10% w/v concentration with lower concentration showed smaller variability among replicates, which tended to be more uniform respect to the other condition, leading to improved consistency of data.

Type A GelMA Medium DoF at 10% w/v concentration enhanced proliferation suggesting how softness matrices positively impact on cellular development. A study on the effect of GelMA based hydrogels' synthesis parameters on cell cultures in fact, demonstrates that low polymer concentrations are essential to provide more favourable microenvironments for the development of cells, achieving optimal levels of viability [43].

These preliminary results were confirmed by subsequent morphological analyses based on digital microscopy, carried out for all the five mCRC patient-derived organoids after 14 days of 3D culture in type A GelMA Medium DoF at 10% and 12,5% w/v concentration. Organoids exhibited greater growth in size when cultured in the lower concentration of GelMA hydrogels, showing typical well-defined spheroidal morphologies in contrast to more heterogeneous shapes whit uneven borders found in the other formulation (Fig.). Therefore, samples cultured in GelMA at 10% w/v concentration revealed greater tendency in mimicking the tissue architecture, resembling the *in vivo* organization of the native organ. Distinct intestinal-like structures as central lumen, cavity spontaneously formed by cell differentiation and apico-basolateral polarization, were found in some samples. In contrast, samples developed in GelMA at 12,5% w/v concentration never featured this characteristic, indicating hydrogel reduced suitability in supporting appropriate organoids growth and organization (Figure 32).
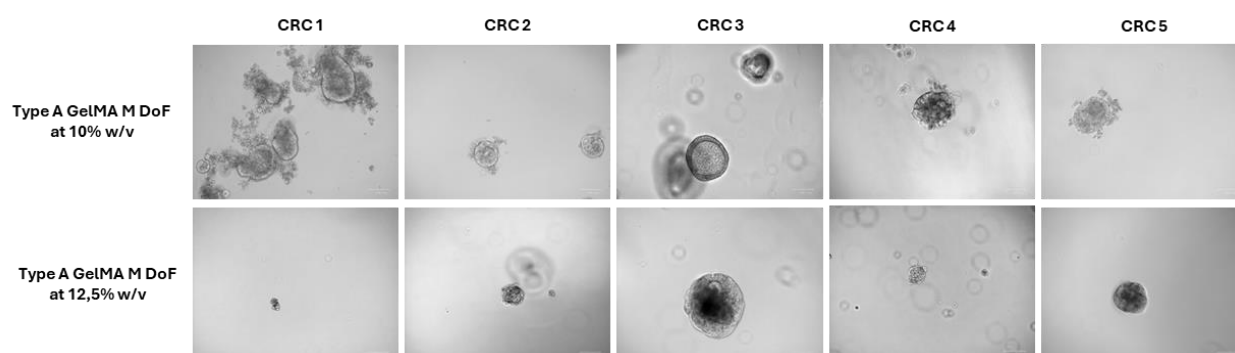

Figure 32: Brightfield microscopy images comparing mCRC patient-derived organoids of culture in type A GelMA Medium DoF at 10% (above) and 12,5% (under) w/v concentrations, at day 14 of 3D culture. (M: Medium, Scale bar: 100 μm).

Although type A GelMA Medium DoF at 10% w/v concentration demonstrated improved performances, it did not always sustain the development of complex structures such as those previously discussed and proliferation must be more optimize. Consequently, further experiments were conducted to evaluate an additional type A GelMA formulation, characterized by the same DoF but lowering the concentration to 7,5% w/v. Reduced polymer concentration led to a decrease in the Young Modulus of the matrix which consequently exhibited limited rigidity and greater elasticity compared to the other GelMA-based hydrogels, making morphological and proliferation performance better.

3.2.2. Type A GelMA Medium DoF at 10% versus 7,5% w/v concentration

3D cultures of the five patient-derived mCRC organoids were performed within type A GelMA Medium DoF hydrogels at 10% and 7,5% w/v concentrations and in Matrigel to investigate organoids proliferation after 7 and 14 days of 3D culture.
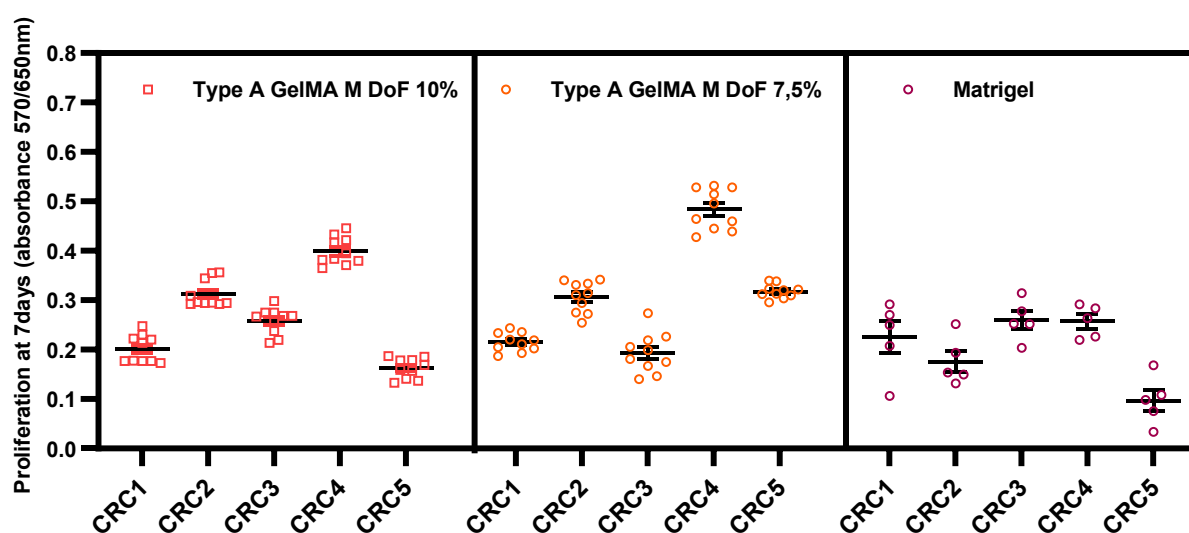

Figure 33: Proliferation rates of the five mCRC patient-derived organoids cultured in type A GelMA Medium DoF at 10% and 7,5% w/v concentrations and in Matrigel, at day 7 of 3D culture. Absorbance values are normalized against the blank. (n= 10 for GelMA and n=5 for Matrigel).

As shown in Figure 33, after 7 days of 3D culture, organoids proliferation in GelMA-based hydrogel at 7,5% w/v concentration was characterized by higher rates compared to the other second formulation in 4 out 5 patients, CRC 1, 2, 4, 5, highlighting improved cellular development in matrix with reduce polymer concentration. Instead, proliferation trends in Matrigel at the same time point, displayed lower values compared with GelMA, for 3 out 5 patients: CRC 2, 4, 5. In particular, for CRC 4 the average proliferation fold increases between values recorded in GelMA and in Matrigel resulted 1.6 and 1.9 for GelMA at 10% and 7,5% w/v concentration, respectively. A similar behaviour was displayed by CRC 5 with an increment of the average proliferation of 1.7

for GelMA at 10% w/v concentration and of 3.3 for GelMA at 7,5% w/v concentration, compared to Matrigel. Moreover, no significant differences in proliferation were observed among the three matrices for CRC 1 and 3.

Live/Dead assay of the organoids was conducted after 7 and 14 days of 3D culture in type A GelMA Medium DoF hydrogel at 7,5% w/v concentration and in Matrigel. Confocal imagining highlighted a complete absence of cell death in samples cultured in both matrices at the two time points (Figure 34), underlying no substantial differences between the two culture conditions. Viable cells (green) population was high with a distribution more or less homogeneous depending on both matrix composition and organoid line considered, demonstrating GelMA compatibility with cellular survival.
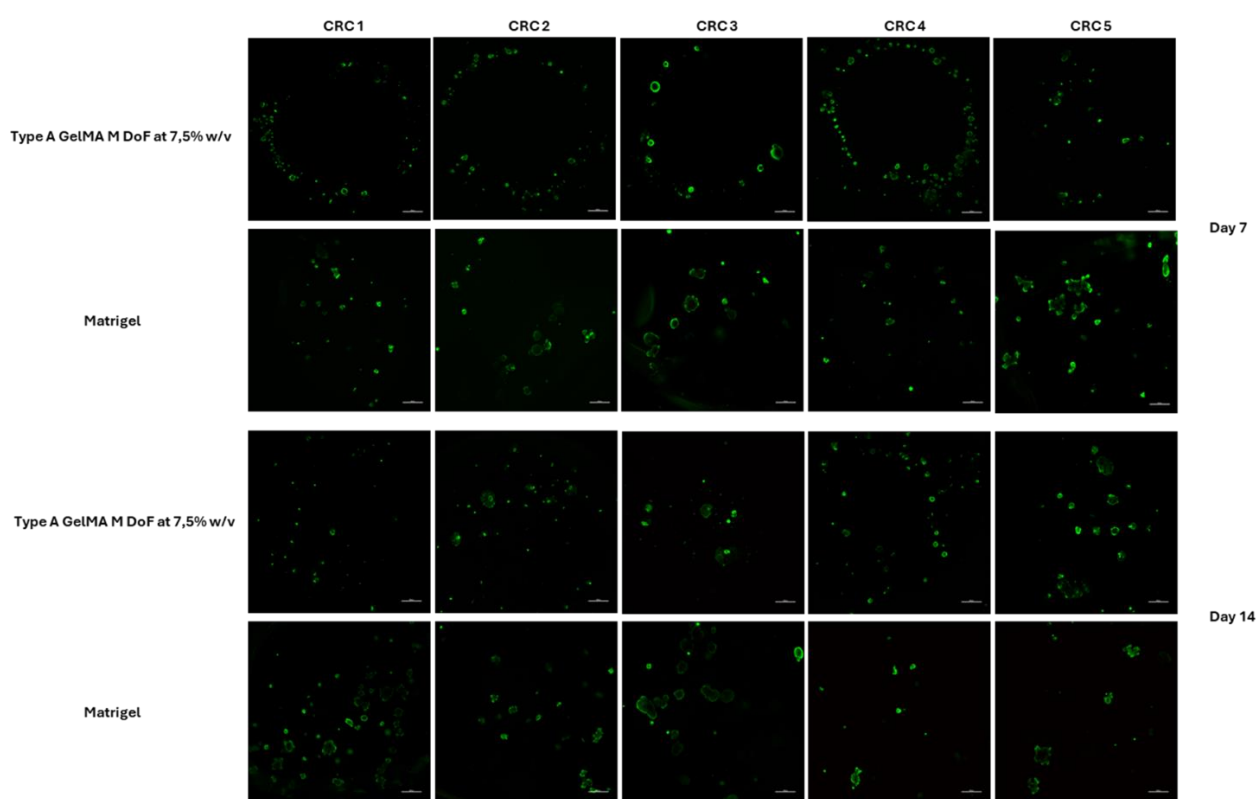

Figure 34: Representative pictures of Live/Dead staining (4X objective lens) showing the viability of the five mCRC patient-derived organoids grown in type A GelMA Medium DoF hydrogel at 7,5% w/v concentration and in Matrigel, at day 7 and 14 of 3D culture. (Scale bar: 500 μm).

After 14 days of 3D culture, 4 out of 5 patient-derived organoids proliferation outperformed in Matrigel despite to GelMA, while CRC 5 displayed higher proliferation in GelMA at 7,5% w/v concentration. Instead, proliferation in type A GelMA Medium DoF at 10% and 7,5% w/v resulted similar for all patient-derived organoids to the one of day 7, without a substantial increase.
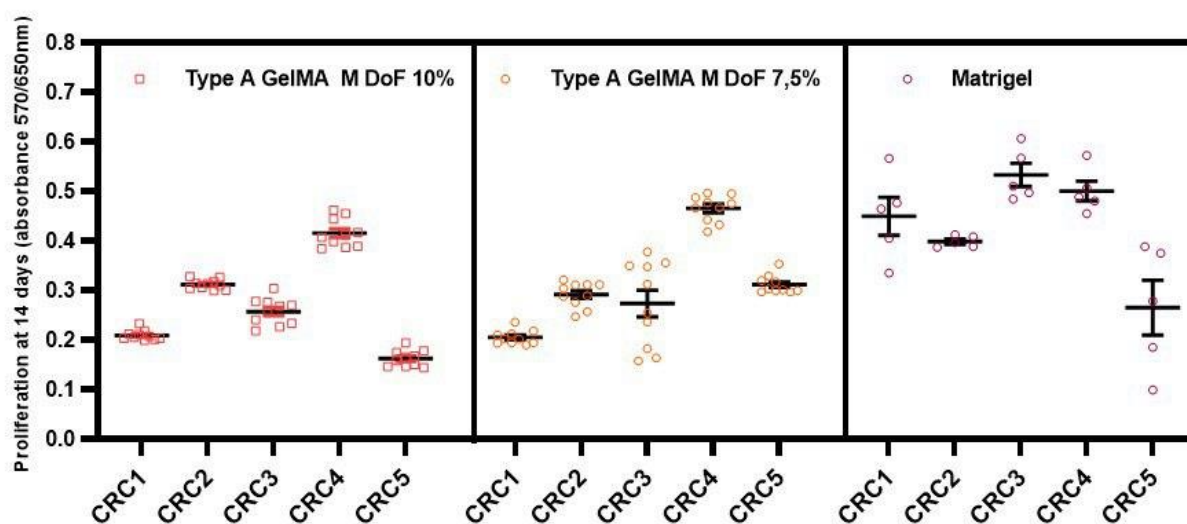

Figure 35: Proliferation rates of the five mCRC patient-derived organoids cultured in type A GelMA Medium DoF at 10% and 7,5% w/v concentrations and in Matrigel, at day 14 of 3D culture. Absorbance values are normalized against the blank. (n= 10 for GelMA and n=5 for Matrigel).

According to these analyses, GelMA-based hydrogels performances may be comparable to the gold standard matrix only in the short term, highlighting their currently inability to sustain the advantage previously achieved. A possible explanation of this phenomenon, in addition to the influence of the matrix's physical properties which significantly impact on cellular behaviour, is the lack in GelMA of ECM proteins and biochemical signals that are crucial for supporting organoids growth and organization. A study conducted on the role of antioxidants in tumour organoids development indicates that the concentration of components as N-acetyl cysteine (precursor of intracellular antioxidant glutathione), which was absent in the culture medium used for GelMA synthesis, is directly proportional to proliferation levels and it also contributes to the formation of filled lumens [51]. Thus, employing a complete culture CRC medium, enriched with N-acetyl cysteine, N-2 and B-27 supplements, for the preparation of GelMA-based hydrogels may contribute to reduce differences with Matrigel.

Digital microscopy was employed to investigate organoids morphology in type A GelMA Medium DoF at 10% and 7,5% w/v concentration and in Matrigel, after 7 days of 3D culture. As shown in Figure 36, which reported the most representative organoids, CRC 3 cultivated in GelMA-based hydrogel at 10% w/v concentration, exhibited oriented growth along a preferential direction, lacking defined spatial organization. In contrast, the same sample cultured within GelMA with lower concentration, developed the typical central lumen, which was also observed in Matrigel 3D

culture. Regarding to CRC 4 instead, distinct surface protrusions, which may resemble the villus-crypt architecture of colonic epithelium, were observed both in GelMA at 7,5% w/v concentration and in Matrigel, underlying high degree of tissue-like organization in organoids developed in these two matrices. These features were not identified in the sample cultured in GelMA at 10% w/v concentration, which was rather characterized by the presence of multicellular groups forming small cell cluster, probably associated to its invasive potential. This analysis suggested that hydrogels with lower GelMA concentrations more closely mimic the supportive properties of Matrigel, facilitating lumenogenesis and the development of other physiologically relevant structures.
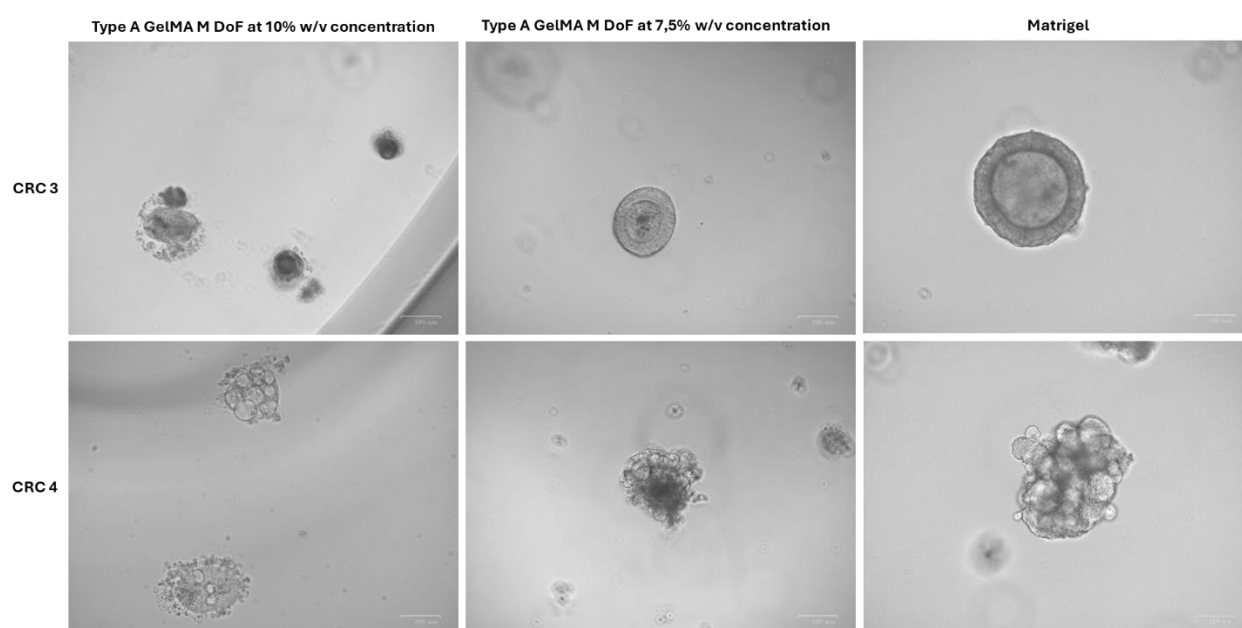

Figure 36: Brightfield microscopy images comparing mCRC patient-derived organoids (CRC 3, 4) grown in type A GelMA Medium DoF hydrogel at 10% and 7,5% w/v concentrations and in Matrigel, at day 7 of 3D culture. (Scale bar: 100 μm).

A more detailed analysis of organoids subcellular components and their organization was performed using DAPI/Phalloidin/WGA staining and confocal microscopy. In Figure 37 a comparison between 14 days of 3D cultures in type A GelMA Medium DoF hydrogel at 10% and 7,5% w/v concentration and in Matrigel, for each organoid is shown. CRC 1 (first line fig.) exhibited a tubular architecture in both GelMA at 7,5% w/v concentration and Matrigel, while in the other GelMA formulation it displayed spherical shape, with no visible intestinal-like structures. Another typical morphological feature of the native tissue was shown by CRC 3 that developed a well-defined central lumen in Matrigel culture, whereas a less pronounced lumen was present in GelMA at 7,5% w/v concentration. Moreover, organoids developed in GelMA at 10% w/v concentration tended to adopt symmetrical organizations while those cultured in GelMA 7,5% w/v concentration and in Matrigel revealed more irregular morphologies, highlighting how reduced

polymer concentration did not induce alterations in the 3D arrangement and better resemble the structural and biochemical features of Matrigel. Regarding to the other samples, no distinct morphological characteristics were distinguished in all three matrices, reflecting the inter-patient variability of the organoids. Moreover, while all the three fluorescence signals were detectable in samples grown in GelMA-based hydrogels, those cultured in Matrigel showed no signals from WGA staining, due to interference issues.
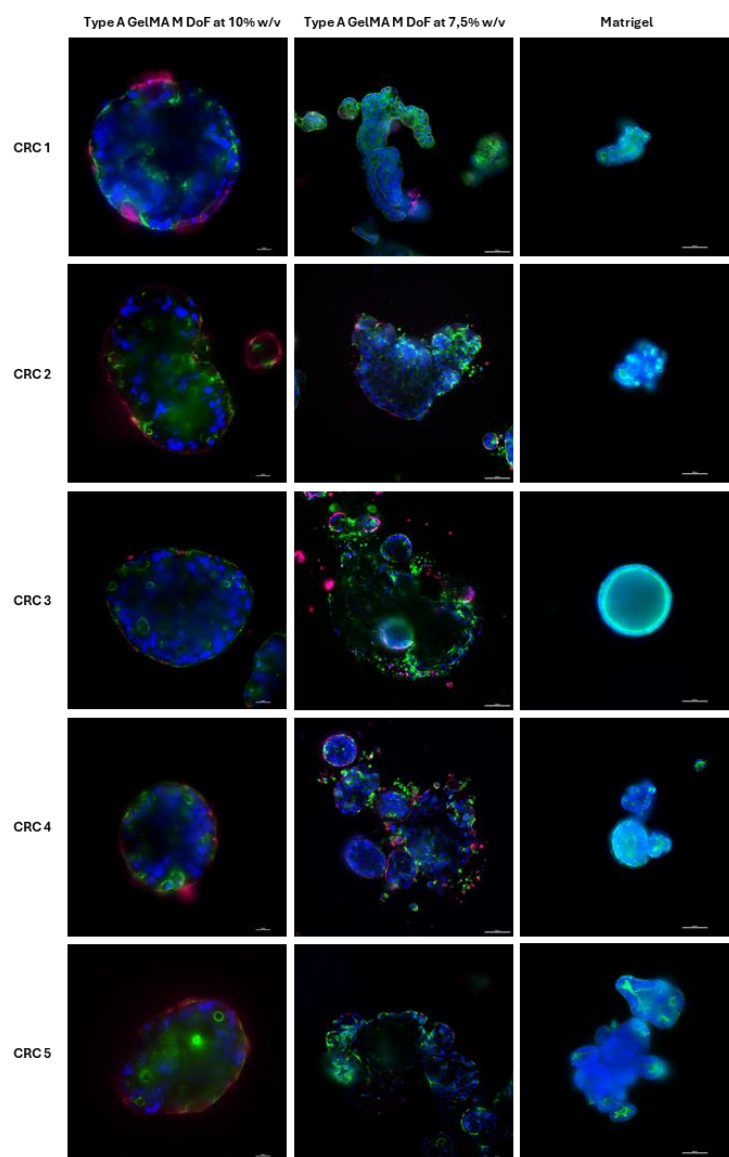

Figure 37: Representative pictures of DAPI-Phalloidin-WGA staining (20X objective lens) showing nuclei (blue), cytoskeleton (green), and plasmatic membrane (pink) of the five mCRC patient-derived organoids cultured in type A GelMA Medium DoF at 10% and 7,5% w/v concentrations and in Matrigel, at day 14 of 3D culture. (M: Medium, Scale bar: 100 μm).

3.3. Drugs response

With the aim to confirm that patient-derived organoids 3D cultured in GelMA and Matrigel showed similar drug response, we performed a preliminary experiment treating them for 72h with Cetuximab (20µg/ml) and Trametinibn (50nM) right after 7 days of 3D culture in type A GelMA Medium DoF at 7,5% w/v concentration and in Matrigel. Organoids from Xenturion Biobank were derived from patients resistant to Cetuximab and during their long-3D culture in Matrigel is confirmed their resistance maintenance [47]. Currently, Trametinib is under evaluation as a therapeutic option for mCRC patients resistant to Cetuximab by the Translational Cancer Medicine Laboratory (Candiolo Cancer Institute), with encouraging preliminary response data. Responses to treatments were evaluated comparing viability of treated organoids with that of untreated ones. As shown in Figure 38, 4 out 5 mCRC patient-derived organoids, CRC 1, 2, 4, 5, confirmed their resistance to Cetuximab treatment both if cultured in GelMA and in Matrigel. When cultured in Matrigel resulted resistant to Cetuximab exposure, CRC 3 cultured in GelMA showed to be sensible to the drug with on average a reduction of the viability of the 60%, if compared to untreated controls. That result, which did not occur for the other patient-derived organoids, can be attributed to experimental artifacts affecting cell viability measurements or sample handling. Although this outcome is presumed to be isolated, its recurrence in future experiments cannot be entirely ruled out, highlighting the importance of further validation to ensure the robustness of the findings. Otherwise, mCRC patient-derived organoids resulted sensible to Trametinib exposure showing a decreasing in cellular viability both in GelMA and Matrigel 3D culture with on average a 31% and a 26% of tumour dead respectively.
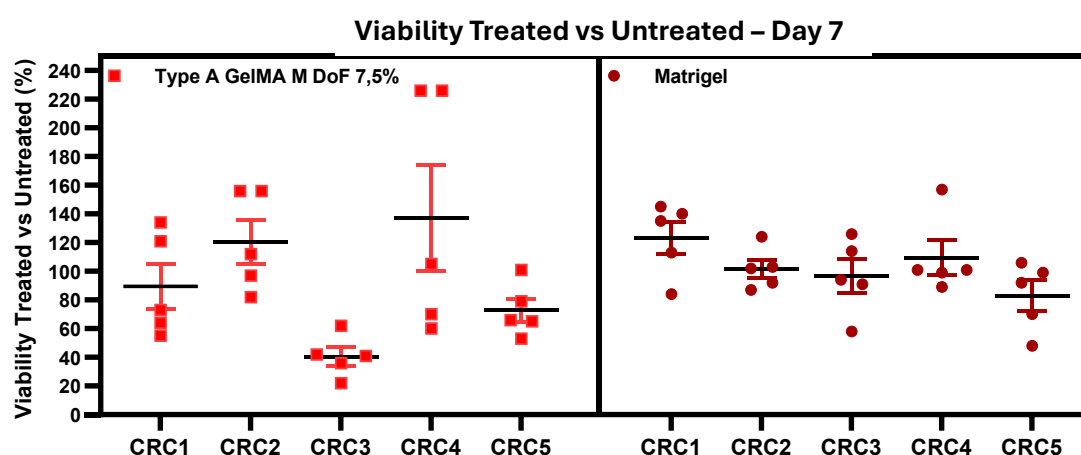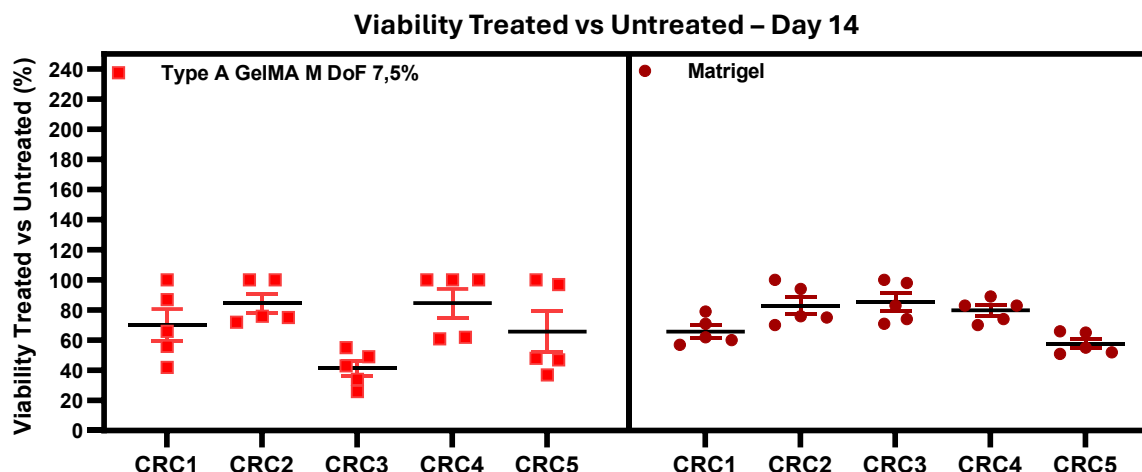
Figure 38: Viability (%) between treated and untreated mCRC patient-derived organoids in type A GelMA Medium DoF at 7,5% w/v concentration and in Matrigel, after 72 hours of Cetuximab and Trametinib exposure.

These comparable results between GelMA and Matrigel based cultures, suggested that GelMA, during 7 days of 3D culture, did not induce significant alterations in cellular drug response respect to the current gold standard matrix.

With the aim to enable morphological comparison between treated and untreated organoids, digital microscopy was conducted on samples grown in Type A GelMA Medium DoF at 7,5% w/v concentration at the end of drugs treatment and compared to the untreated ones. In Figure 38 are shown representative pictures of CRC 4, that after the exposure to Cetuximab exhibited increased size if compared to the untreated controls, confirming the results obtained with viability analysis and the resistance to Cetuximab that allows organoids to growth better than controls. The increase in organoid dimensions is generally considered an indicator of a supportive microenvironment, promoting cellular proliferation and organization, and is therefore associated with enhanced viability. On the contrary, organoids treated with Trametinib, displayed reduced size, suggesting a certain sensibility to the drug. These findings highlight the differential response of the organoids to the two treatments and reinforce the relevance of morphological evaluation as a complementary approach to viability-based assays.
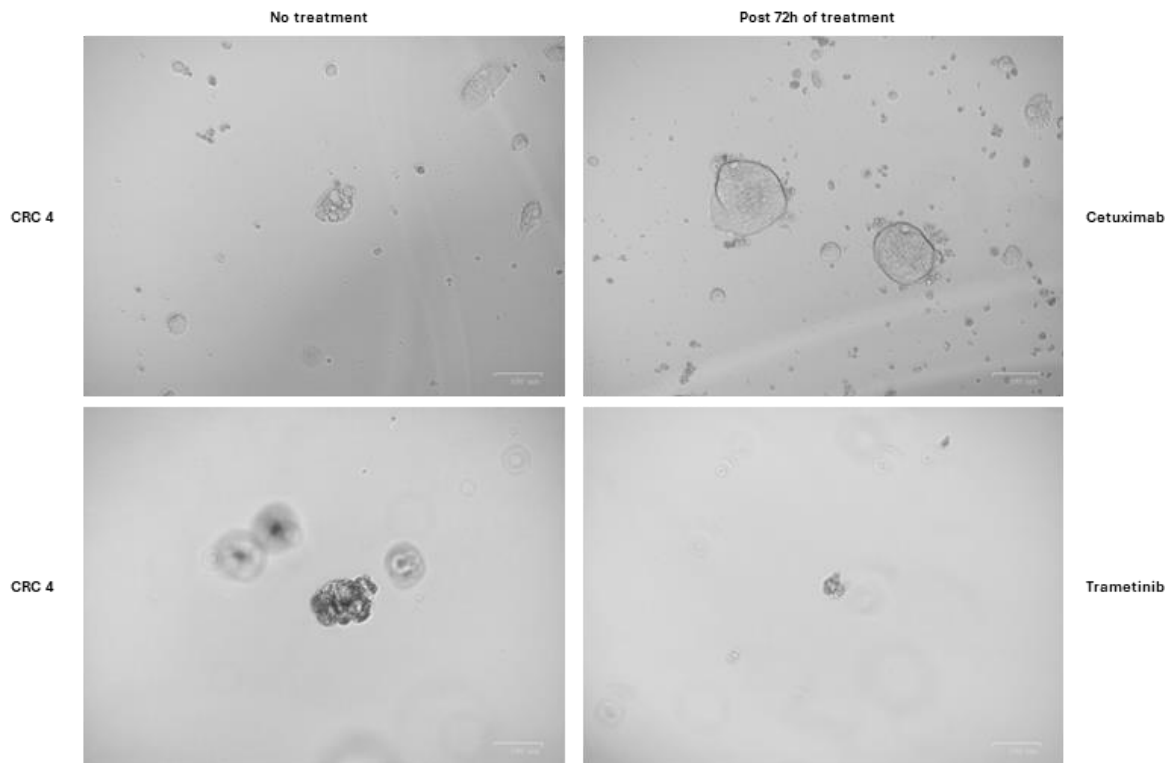
Figure 39: Brightfield microscopy comparing untreated (on the left) with treated (on the right) CRC 4 patient-derived organoids, after 72 hours of Cetuximab and Trametinib treatment. All the samples are grown in type A GelMA Medium DoF hydrogel at 7,5% w/v concentration. (Scale bar: 100 μm)

4. Conclusion

GelMA-based hydrogels represent promising 3D systems for multiple biomedical applications due to their remarkable characteristics as biocompatibility and mechanical tunability. The aim of this thesis was to develop and validate a GelMA-based hydrogel for 3D culture of mCRC patient-derived organoids, shared by XENTURION Biobank of Candiolo Cancer Institute, as a potential alternative to Matrigel, the current gold standard. By varying GelMA type (A and B) and synthesis parameters, namely the DoF (High and Medium) and the percentages of polymer concentration (12,5%, 10%, and 7,5% w/v), different hydrogel formulation were evaluated. This optimization aim to identify the best condition that support adequate organoids proliferation and proper morphological organisation. Finally, two drugs (Cetuximab and Trametinib) were tested on the most promising GelMA formulation to assess whether culturing organoids in GelMA could lead to alterations in drug response compared to Matrigel.

Firstly, the most suitable GelMA type for culturing T84 mCRC commercial cell line, was selected between type A and B, both characterized by High DoF and 12,5% w/v concentration. Type A supported greater cell proliferation at day 7, probably due to the positive charges exposed by its functional groups at physiological pH, which promote cell–matrix interactions. Subsequently, the impact of changing the DoF from High to Medium was evaluated on T84 cells proliferation and morphology. It was observed that the Medium DoF not only promoted a greater cellular growth between day 7 and day 14 (increment of 52%) but also resulted in improved structural organization and increased cellular size. After selecting the type and the DoF of GelMA hydrogel, three different polymer concentrations, namely 12,5%, 10% and 7,5% w/v, were evaluated to assess their impact on organoids development. The comparison between the first two concentrations revealed that GelMA at 10% w/v created a more favourable microenvironment, promoting a general increase in organoids proliferation over time. Moreover, in some cases the organoids cultured in GelMA at 10% w/v exhibited a central lumen, one of the most representative features of intestinal architecture. However, GelMA-based hydrogels at 10% w/v concentration did not consistently support the formation of complex structures reproducing the native tissue, which instead are clearly observed in the GelMA at 7,5% w/v concentration. This latter formulation did not induce alterations in the 3D arrangement of organoids that exhibited central lumen, tube-like structures and superficial protrusions resembling the villus-crypt organization. All these morphologies were observed also in Matrigel, suggesting how the reduction of the polymer concentration results in microenvironments which more closely replicates the supportive properties of the gold standard matrix. Although proliferation at day 14 of 3D culture resulted higher in Matrigel for 4 out 5 samples, likely due to the absence of essential growth factors and supplements in the culture

medium used for hydrogels synthesis, GelMA at 7,5% w/v concentration showed superior proliferation capability compared to the formulation at 10% w/v. These results were also confirmed by viability assays conducted over 7 and 14 days of culture. Therefore, GelMA Medium DoF at 7,5% w/v concentration was employed to study of organoids sensibility to Cetuximab and Trametinib. Both cell viability and morphological analyses, conducted 72 hours after drugs administration, revealed that 4 out 5 organoids were resistant to Cetuximab in both matrices, showing increased size in treated samples. In contrast, treatment with Trametinib resulted in greater sensitivity, with reduced organoids viability and dimension both in Matrigel and GelMA-based hydrogel.

These analyses confirm that GelMA type A can be considered a reliably alternative to conventional matrices for 3D organoids culture, offering performances that are comparable to Matrigel in terms of proliferative capability and morphological characterization.

Nevertheless, the model proposed in this thesis, still presents several limitations, primarily related to the lack of biological signals and ECM components which negatively affect the proliferation at 14 days when compared to the current gold standard. Future developments will include the use of complete culture medium for GelMA synthesis, transcriptomic analyses to investigate the degree of correspondence between the mutational profiles of organoids cultured in GelMA and the original tumours, but also the integration of other cellular phenotypes to enhance the complexity and physiological relevance of the model.

Bibliography

[1]   C. Yang *et al.*, "Tumor organoid model of colorectal cancer (Review)," *Oncol Lett*, vol. 26, no. 2, 2023, doi: 10.3892/ol.2023.13914.

[2]   R. Deshmukh, M. Prajapati, and R. K. Harwansh, "A review on emerging targeted therapies for the management of metastatic colorectal cancers," 2023. doi: 10.1007/s12032-023-02020-x.

[3]   V. A. Ionescu, G. Gheorghe, N. Bacalbasa, A. L. Chiotoroiu, and C. Diaconu, "Colorectal Cancer: From Risk Factors to Oncogenesis," 2023. doi: 10.3390/medicina59091646.

[4]   R. AHMAD, J. K. SINGH, A. WUNNAVA, O. AL-OBEED, M. ABDULLA, and S. K. SRIVASTAVA, "Emerging trends in colorectal cancer: Dysregulated signaling pathways (Review)," 2021. doi: 10.3892/ijmm.2021.4847.

[5]   L. H. Biller and D. Schrag, "Diagnosis and treatment of metastatic colorectal cancer: A review," 2021. doi: 10.1001/jama.2021.0106.

[6]   P. W. Underwood, S. M. Ruff, and T. M. Pawlik, "Update on Targeted Therapy and Immunotherapy for Metastatic Colorectal Cancer," 2024. doi: 10.3390/cells13030245.

[7]   J. Li, X. Ma, D. Chakravarti, S. Shalapour, and R. A. DePinho, "Genetic and biological hallmarks of colorectal cancer," 2021. doi: 10.1101/gad.348226.120.

[8]   K. He *et al.*, "Metastasis organotropism in colorectal cancer: advancing toward innovative therapies," 2023. doi: 10.1186/s12967-023-04460-5.

[9]   S. M. Ruff and T. M. Pawlik, "A Review of Translational Research for Targeted Therapy for Metastatic Colorectal Cancer," 2023. doi: 10.3390/cancers15051395.

[10]   M. Riihimaki, A. Hemminki, J. Sundquist, and K. Hemminki, "Patterns of metastasis in colon and rectal cancer," *Sci Rep*, vol. 6, 2016, doi: 10.1038/srep29765.

[11]   G. Zhu, L. Pei, H. Xia, Q. Tang, and F. Bi, "Role of oncogenic KRAS in the prognosis, diagnosis and treatment of colorectal cancer," 2021. doi: 10.1186/s12943-021-01441-4.

[12]   R. B. Corcoran *et al.*, "Combined BRAF, EGFR, and MEK Inhibition in Patients With BRAFV600E -Mutant Colorectal Cancer," *Cancer Discov*, vol. 8, no. 4, 2018.

[13]   R. B. Corcoran *et al.*, "Combined BRAF and MEK inhibition with dabrafenib and trametinib in BRAF V600-Mutant colorectal cancer," in *Journal of Clinical Oncology*, 2015. doi: 10.1200/JCO.2015.63.2471.

[14]   E. Reidy, N. A. Leonard, O. Treacy, and A. E. Ryan, "A 3D view of colorectal cancer models in predicting therapeutic responses and resistance," *Cancers (Basel)*, vol. 13, no. 2, 2021, doi: 10.3390/cancers13020227.

[15]   N. Manduca, E. Maccafeo, R. De Maria, A. Sistigu, and M. Musella, "3D cancer models: One step closer to in vitro human studies," 2023. doi: 10.3389/fimmu.2023.1175503.

[16]   W. H. Abuwatfa, W. G. Pitt, and G. A. Husseini, "Scaffold-based 3D cell culture models in cancer research," 2024. doi: 10.1186/s12929-024-00994-y.

[17]   C. Corrò, L. Novellasdemunt, and V. S. W. Li, "A brief history of organoids," *Am J Physiol Cell Physiol*, vol. 319, no. 1, 2020, doi: 10.1152/ajpcell.00120.2020.

[18]   E. C. Anderson, C. Hessman, T. G. Levin, M. M. Monroe, and M. H. Wong, "The role of colorectal cancer stem cells in metastatic disease and therapeutic response," 2011. doi: 10.3390/cancers3010319.

[19]   T. Sato *et al.*, "Long-term expansion of epithelial organoids from human colon, adenoma, adenocarcinoma, and Barrett's epithelium," *Gastroenterology*, vol. 141, no. 5, 2011, doi: 10.1053/j.gastro.2011.07.050.

[20]   J. Lv, X. Du, M. Wang, J. Su, Y. Wei, and C. Xu, "Construction of tumor organoids and their application to cancer research and therapy," 2024. doi: 10.7150/thno.91362.

[21]   M. Taglieri *et al.*, "Colorectal Organoids: Models, Imaging, Omics, Therapy, Immunology, and Ethics," Mar. 01, 2025, *Multidisciplinary Digital Publishing Institute (MDPI)*. doi: 10.3390/cells14060457.

[22]   K. yu Zhao, Y. xiang Du, H. min Cao, L. ya Su, X. lan Su, and X. Li, "The Biological Macromolecules constructed Matrigel for cultured organoids in biomedical and tissue engineering," Mar. 01, 2025, *Elsevier B.V.* doi: 10.1016/j.colsurfb.2024.114435.

[23]   A. Passaniti, H. K. Kleinman, and G. R. Martin, "Matrigel: history/background, uses, and future applications," 2022. doi: 10.1007/s12079-021-00643-1.

[24]   M. T. Kozlowski, C. J. Crook, and H. T. Ku, "Towards organoid culture without Matrigel," 2021. doi: 10.1038/s42003-021-02910-8.

[25]   O. Habanjar, M. Diab-Assaf, F. Caldefie-Chezet, and L. Delort, "3D cell culture systems: Tumor application, advantages, and disadvantages," 2021. doi: 10.3390/ijms222212200.

[26]   E. A. Aisenbrey and W. L. Murphy, "Synthetic alternatives to Matrigel," 2020. doi: 10.1038/s41578-020-0199-8.

[27]   B. Y. Xie and A. W. Wu, "Organoid culture of isolated cells from patient-derived tissues with colorectal cancer," *Chin Med J (Engl)*, vol. 129, no. 20, 2016, doi: 10.4103/0366-6999.191782.

[28]   F. K. Braun *et al.*, "Scaffold-Based (Matrigel^{TM}) 3D Culture Technique of Glioblastoma Recovers a Patient-like Immunosuppressive Phenotype," *Cells*, vol. 12, no. 14, 2023, doi: 10.3390/cells12141856.

[29]   S. Kim *et al.*, "Tissue extracellular matrix hydrogels as alternatives to Matrigel for culturing gastrointestinal organoids," *Nat Commun*, vol. 13, no. 1, 2022, doi: 10.1038/s41467-022-29279-4.

[30]   D. Loessner *et al.*, "Functionalization, preparation and use of cell-laden gelatin methacryloyl-based hydrogels as modular tissue culture platforms," *Nat Protoc*, vol. 11, no. 4, 2016, doi: 10.1038/nprot.2016.037.

[31]   T. C. Ho *et al.*, "Hydrogels: Properties and Applications in Biomedicine," 2022. doi: 10.3390/molecules27092902.

[32]   H. Cao, L. Duan, Y. Zhang, J. Cao, and K. Zhang, "Current hydrogel advances in physicochemical and biological response-driven biomedical application diversity," 2021. doi: 10.1038/s41392-021-00830-x.

[33]   L. Lu *et al.*, "The Formation Mechanism of Hydrogels," *Curr Stem Cell Res Ther*, vol. 13, no. 7, 2017, doi: 10.2174/1574888x12666170612102706.

[34]   W. Hu, Z. Wang, Y. Xiao, S. Zhang, and J. Wang, "Advances in crosslinking strategies of biomedical hydrogels," 2019. doi: 10.1039/c8bm01246f.

[35]   N. Sood, A. Bhardwaj, S. Mehta, and A. Mehta, "Stimuli-responsive hydrogels in drug delivery and tissue engineering," 2016. doi: 10.3109/10717544.2014.940091.

[36] K. Yue, G. Trujillo-de Santiago, M. M. Alvarez, A. Tamayol, N. Annabi, and A. Khademhosseini, "Synthesis, properties, and biomedical applications of gelatin methacryloyl (GelMA) hydrogels," 2015. doi: 10.1016/j.biomaterials.2015.08.045.

[37] B. H. Lee, N. Lum, L. Y. Seow, P. Q. Lim, and L. P. Tan, "Synthesis and characterization of types A and B gelatin methacryloyl for bioink applications," *Materials*, vol. 9, no. 10, 2016, doi: 10.3390/ma9100797.

[38] C. E. Campiglio, N. C. Negrini, S. Farè, and L. Draghi, "Cross-linking strategies for electrospun gelatin scaffolds," 2019. doi: 10.3390/ma12152476.

[39] C. G. Gaglio, D. Baruffaldi, C. F. Pirri, L. Napione, and F. Frascella, "GelMA synthesis and sources comparison for 3D multimaterial bioprinting," *Front Bioeng Biotechnol*, vol. 12, 2024, doi: 10.3389/fbioe.2024.1383010.

[40] N. V. Arguchinskaya *et al.*, "Properties and Printability of the Synthesized Hydrogel Based on GelMA," *Int J Mol Sci*, vol. 24, no. 3, 2023, doi: 10.3390/ijms24032121.

[41] A. G. Kurian, R. K. Singh, K. D. Patel, J. H. Lee, and H. W. Kim, "Multifunctional GelMA platforms with nanomaterials for advanced tissue therapeutics," 2022. doi: 10.1016/j.bioactmat.2021.06.027.

[42] S. Bupphathong, C. Quiroz, W. Huang, P. F. Chung, H. Y. Tao, and C. H. Lin, "Gelatin Methacrylate Hydrogel for Tissue Engineering Applications—A Review on Material Modifications," 2022. doi: 10.3390/ph15020171.

[43] I. Pepelanova, K. Kruppa, T. Scheper, and A. Lavrentieva, "Gelatin-methacryloyl (GelMA) hydrogels with defined degree of functionalization as a versatile toolkit for 3D cell culture and extrusion bioprinting," *Bioengineering*, vol. 5, no. 3, 2018, doi: 10.3390/bioengineering5030055.

[44] R. N. Ghosh *et al.*, "An insight into synthesis, properties and applications of gelatin methacryloyl hydrogel for 3D bioprinting," 2023. doi: 10.1039/d3ma00715d.

[45] D. Duymaz, İ. C. Karaoğlu, and S. Kizilel, "Effect of Photoinitiation Process on Photo-Crosslinking of Gelatin Methacryloyl Hydrogel Networks," Apr. 16, 2025. doi: 10.1101/2025.04.10.648118.

[46] S. Sharifi, H. Sharifi, A. Akbari, and J. Chodosh, "Systematic optimization of visible light-induced crosslinking conditions of gelatin methacryloyl (GelMA)," *Sci Rep*, vol. 11, no. 1, 2021, doi: 10.1038/s41598-021-02830-x.

[47] S. M. Leto *et al.*, "XENTURION is a population-level multidimensional resource of xenografts and tumoroids from metastatic colorectal cancer patients," *Nature Communications* , vol. 15, no. 1, Dec. 2024, doi: 10.1038/s41467-024-51909-2.

[48] M. Ghasemi, T. Turnbull, S. Sebastian, and I. Kempson, "The mtt assay: Utility, limitations, pitfalls, and interpretation in bulk and single-cell analysis," *Int J Mol Sci*, vol. 22, no. 23, 2021, doi: 10.3390/ijms222312827.

[49] K. J. Goudie, S. J. McCreath, J. A. Parkinson, C. M. Davidson, and J. J. Liggat, "Investigation of the influence of pH on the properties and morphology of gelatin hydrogels," *Journal of Polymer Science*, vol. 61, no. 19, 2023, doi: 10.1002/pol.20230141.

[50] I. Pepelanova, K. Kruppa, T. Scheper, and A. Lavrentieva, "Gelatin-methacryloyl (GelMA) hydrogels with defined degree of functionalization as a versatile toolkit for 3D cell culture and extrusion bioprinting," *Bioengineering*, vol. 5, no. 3, 2018, doi: 10.3390/bioengineering5030055.